




**BULGARIAN ACADEMY OF SCIENCES**

**The Stephan Angeloff Institute of Microbiology**

**Nikola Ralchev Ralchev**

# *Suppression of antigen-specific B lymphocytes through protein engineering molecules in hypersensitivity reactions*

# ABSTRACT

of a dissertation for awarding the educational and scientific degree PhD in a professional direction 4.3. Biological Sciences, Scientific specialty "Immunology"

**Research supervisor: Prof. Andrey Tchorbanov, PhD**

**Sofia 2025**

The current dissertation was developed at the Department of Immunology, Laboratory of Experimental Immunology, " Stephan Angeloff " Institute of Microbiology, BAS.

The dissertation consists of 106 pages, 2 tables and includes 29 figures. The bibliography comprises 211 literary sources.

The dissertation was discussed and directed for defense at a meeting of the National Seminar held by the Department of Immunology at the Stefan Angelov Institute of Microbiology, Bulgarian Academy of Sciences.

The defense of the dissertation will take place during an open session in front of a scientific jury on ..... at ..... hours in the hall of the Institute of Microbiology "Stefan Angelov", BAS, ul. "Akad. G. Bonchev", bl. 26, Sofia. Materials related to the defense are available in the office of the scientific secretary of the Institute and have been published in accordance with the Law on the Protection of Scientific and Technological Information of the Republic of Bulgaria at www.microbio.bas.bg.

**BULGARIAN ACADEMY OF SCIENCES**

**The Stephan Angeloff Institute of Microbiology**

**Nikola Ralchev Ralchev**

# *Suppression of antigen-specific B lymphocytes through protein engineering molecules in hypersensitivity reactions*

# ABSTRACT

of a dissertation for awarding the educational and scientific degree PhD in a professional direction 4.3. Biological Sciences, Scientific specialty "Immunology"

**Research supervisor: Prof. Andrey Tchorbanov, PhD**

Scientific jury:

Assoc. Prof. Petya Dimitrova, PhD

Prof. Krassimira Todorova, PhD

Assoc. Prof. Nikolina Mihaylova, PhD

Assoc. Prof. Ekaterina Ivanova, PhD

Assoc. Prof. Ivanka Tsacheva, PhD

# ABBREVIATIONS

| | |
|---|---|
| ADCC | Antibody-dependent cellular cytotoxicity |
| AIT | Allergen immunotherapy |
| Alum | Aluminium hydroxide, $Al(OH)_3$ |
| APC | Allophycocyanin |
| BAD | BCL-2 associated agonist of cell death |
| BAL | bronchoalveolar lavage |
| BALF | bronchoalveolar lavage fluid |
| BCL | B-cell lymphoma |
| BCR | B-cell receptor |
| BID | BH3 Interacting Domain Death Agonist |
| BSA | bovine serum albumin |
| CR1 | Complement receptor 1, CD35 |
| DC-SIGN | dendritic cell specific ICAM-3-grabbing non-integrin |
| Dpt | *Dermatophagoides pteronyssinus* |
| ELISA | enzyme-linked immunosorbent assay |
| FACS | fluorescence-activated cell sorting |
| FcγRIIb | Fc fragment of IgG receptor IIb |
| FcεRI | high-affinity Fc receptor for IgE |
| FITC | Fluorescein isothiocyanate |
| GM-CSF | granulocyte-macrophage colony-stimulating factor |
| H&E | Hematoxylin and Eosin |
| HDM | house dust mites |
| HRP | Horseradish Peroxidase |
| i.n. | intranasal |
| i.p. | intraperitoneal |
| i.v. | intravenous |
| IgE | Immunoglobulin E |
| IL | interleukin |
| IL4R | Interleukin 4 Receptor |

| | |
|---|---|
| ITAM | immunoreceptor tyrosine-based activation motif |
| ITIM | immunoreceptor tyrosine-based inhibition motif |
| JNK | c-Jun N-terminal kinase |
| LPS | lipopolysaccharides |
| MAPKs | mitogen-activated protein kinases |
| MBP | major basic protein |
| MHCII | major histocompatibility complex class II |
| MyD88 | Myeloid Differentiation Primary Response Protein 88 |
| NF-κB | Nuclear factor kappa B |
| NK клетки | natural killer cells |
| NLRs | nucleotide-binding and oligomerization domain (NOD)-like receptors |
| NOD | nucleotide-binding and oligomerization domain |
| NOD-SCID | Nonobese diabetic - severe combined immunodeficiency |
| ON | overnight |
| PAF | platelet-activating factor |
| PAMPs | pathogen-associated molecular patterns |
| PARs | protease-activated receptors |
| PBMCs | peripheral blood mononuclear cells |
| PBS | phosphate-buffered saline |
| PE | phycoerythrin |
| PeCy7 | phycoerythrin-cyanine7 |
| PRRs | Pattern Recognition Receptors |
| rpm | revolutions per minute |
| RT | room temperature |
| SCF | stem cell factor |
| SCID | severe combined immunodeficiency |
| SCIT | subcutaneous immunotherapy |
| SHIP | SH2 domain-containing inositol phosphatase |
| SLIT | sublingual immunotherapy |

| | |
|---|---|
| SNP | Single Nucleotide Polymorphism |
| SPF | specific pathogen-free |
| STAT6 | signal transducer and activator of transcription 6 |
| Th2 | T helper 2 cells |
| TMB | 3,3′,5,5′-tetramethylbenzidine |
| TNF-α, β | tumor necrosis factor α and β |
| T-PBS | 0.05% Tween 20 in PBS |
| TSLP | thymic stromal lymphopoietin |
| VDBP | Vitamin D Binding Protein |
| VDR | Vitamin D Receptor |

# I. INTRODUCTION

Type I hypersensitivity reactions, also known as allergic reactions, develop as a result of an immune response to harmless environmental antigens, referred to as allergens. These reactions are rapid and mediated by allergen-specific IgE antibodies, which bind to receptors on the surface of effector cells. Subsequent binding of the allergen to these IgE antibodies triggers degranulation and the release of histamine and other bioactive molecules from the effector cells.

Allergic reactions are widespread, and the pathology of these diseases depends on the site of allergen entry. House dust mites (HDM) are the most common triggers of respiratory allergies, causing allergic rhinitis and allergic asthma. Allergic inflammation in these patients leads to significant impairment of their productivity and well-being, associated with high public expenditures and the need for costly and prolonged therapy.

The management of allergic diseases typically involves allergen avoidance and pharmacological treatment aimed at alleviating disease symptoms. However, symptomatic relief of HDM allergy ceases once treatment is discontinued or the patient is re-exposed to the allergen. Allergen-specific immunotherapy (AIT) is the only established treatment targeting the fundamental allergic mechanisms, providing long-term benefits. Nevertheless, AIT requires lengthy protocols, usually lasting 3–4 years, and there is uncertainty regarding its cost-effectiveness and long-term efficacy. Thus, innovative therapeutic approaches are needed to improve the long-term management of HDM allergies.

Der p 1 is one of the major allergens responsible for HDM allergy. The critical role of IgE antibodies highlights Der p 1-specific B cells as a logical target for HDM allergy treatment. A novel therapeutic approach leading to the selective elimination of allergen-specific B cells could be considered a potential treatment for the disease. Potential targets for such selective therapy include the B-cell receptor (BCR) in combination with inhibitory receptors on the surface of B cells, such as the human complement receptor 1 (CR1) and the murine receptor FcγRIIb.

# II. AIM AND OBJECTIVES

The aim of the present dissertation is to selectively suppress the production of allergen-specific antibodies in murine and humanized models of house dust mite allergy through therapy with chimeric molecules containing a monoclonal antibody against an inhibitory receptor (human CR1 or murine FcγRIIb), conjugated to an epitope-bearing peptide p52-71 from *Dermatophagoides pteronyssinus*.

To achieve this aim, the following objectives were set:

1. Construction and characterization of the murine Dp52-71 chimera.
2. Development of experimental models of house dust mite allergy:

2.1. A humanized Rag2- γc- model.

2.2. A murine BALB/c model of chronic allergic inflammation.

3. Administration of chimeric molecules in the experimental allergy models and investigation of their effect on allergen-specific antibody levels.
4. Evaluation of the therapeutic effect of the chimeras on lung damage and the characteristics of the immune response mediated by allergic inflammation in both experimental models.

# III. MATERIALS AND METHODS

## 1. Humanized murine model of house dust mite allergy

### 1.1. Monoclonal antibodies and chimeric molecules

In previous studies, anti-human chimeric molecules were constructed and characterized. Their ability to bind to target receptors was confirmed. These chimeric molecules contain the murine 3D9 IgG1 monoclonal antibody, specific for human CR1, conjugated with either the peptide p52-71 (Ac-NQSLDLAEQELVDCASQHGC-Ahx-K-$NH_2$) from Der p 1 (Dp52-71 chimera) or a control peptide (Ac-DEACLQCGSEDHQAVQNLLS-Ahx-K-$NH_2$) (control chimera), which contains the same amino acids in a different sequence [174].

Fluorescein isothiocyanate (FITC)-conjugated anti-human CD45 (Cat# 0782, clone J.33, Immunotech), anti-human CD3-PeCy7 (Cat# 60-0036-T100, clone SK7, Tonbo Biosciences), anti-human CD4-APC (Cat# 17-0048-42, clone OKT4, eBiosciences), anti-human CD19-eFluor450 (Cat# 48-0198-42, clone SJ25C1, eBiosciences), and phycoerythrin (PE)-conjugated anti-human CD8a (Cat# 12-0088-42, clone RPA-T8, eBiosciences) were used for flow cytometry (FACS) experiments.

### 1.2. Allergic patients

The study included four newly diagnosed, untreated patients with bronchial asthma and/or allergic rhinitis sensitized to *Dermatophagoides pteronyssinus* (Dpt) (female-to-male ratio: 1:3; age range: 16–32 years)

Inclusion criteria for the study were a diagnosis of house dust mite (HDM) allergy established at least two years prior to the study through skin allergy testing and/or flow cytometry (FACS) analysis for basophil degranulation, along with the presence of a high titer of allergen-specific IgE antibodies. Informed consent was obtained from all participants, and the study was conducted in accordance with the Declaration of Helsinki.

Peripheral blood mononuclear cells (PBMCs) from allergic patients were isolated using a density gradient solution, Pancoll (Cat# P04-60225, PAN Biotech, Aidenbach, Germany). Briefly, blood diluted threefold with PBS was carefully layered onto the density gradient, ensuring no mixing of the phases. After centrifugation at 800 × g for 20 minutes at room temperature (RT), the PBMC layer, located between the plasma and Pancoll layers, was collected.

The isolated PBMCs were further purified to remove residual serum, platelets, and Pancoll by two additional washes in phosphate-buffered saline (PBS) via centrifugation at 300 × g for 10 minutes. Viable cells were counted using a Bürker counting chamber with 0.25% trypan blue solution.

### 1.3. Rag2- γc- Mice

Female 8-week-old Rag2-γc- mice (C;129S4-Rag2tm1.1Flv Il2rgtm1.1Flv/J) were purchased from The Jackson Laboratory (Cat# 014593, Bar Harbor, ME). The animals were maintained under specific pathogen-free (SPF) conditions. All procedures were performed in compliance with Directive 2010/63/EU on the protection of animals used for scientific purposes and national regulations.

### 1.4. Cell Transfer

Female Rag2- γc- mice (2 mice per donor, 8 total) were used for the transfer of human cells. PBMCs obtained from *Dermatophagoides pteronyssinus*-sensitized patients were isolated as described above. Cells from each donor were divided into equal parts, and a total of $1 \times 10^7$ cells were transferred intraperitoneally (i.p.) into each Rag2- γc- mouse. A detailed treatment scheme is presented in Figure 1.

### 1.5. Treatment Scheme for the Humanized Rag2- γc- Model of HDM Allergy

Rag2- γc- mice were humanized with PBMCs from allergic patients and divided into two groups. The first group was injected intravenously (i.v.) once a week for 4 weeks with 50 μg of the Dp52-71 chimera per mouse, starting on day 3 after PBMC transfer. The second group was injected with the control chimera following the same schedule.

On days 0 and 17 after the transfer of human PBMCs, the mice were sensitized with 100 μg/mouse of HDM extract (Cat# 02.01.85, Citeq Biologics, Groningen, Netherlands) adsorbed onto 100 μg of alum ($Al(OH)_3$) (kindly provided by the National Center of Infectious and Parasitic Diseases, Sofia, Bulgaria).

Three times per week, after treatment with the chimeras, the mice were anesthetized and stimulated via intranasal administration of 25 μg/mouse of HDM extract in a final volume of 35 μl/mouse.

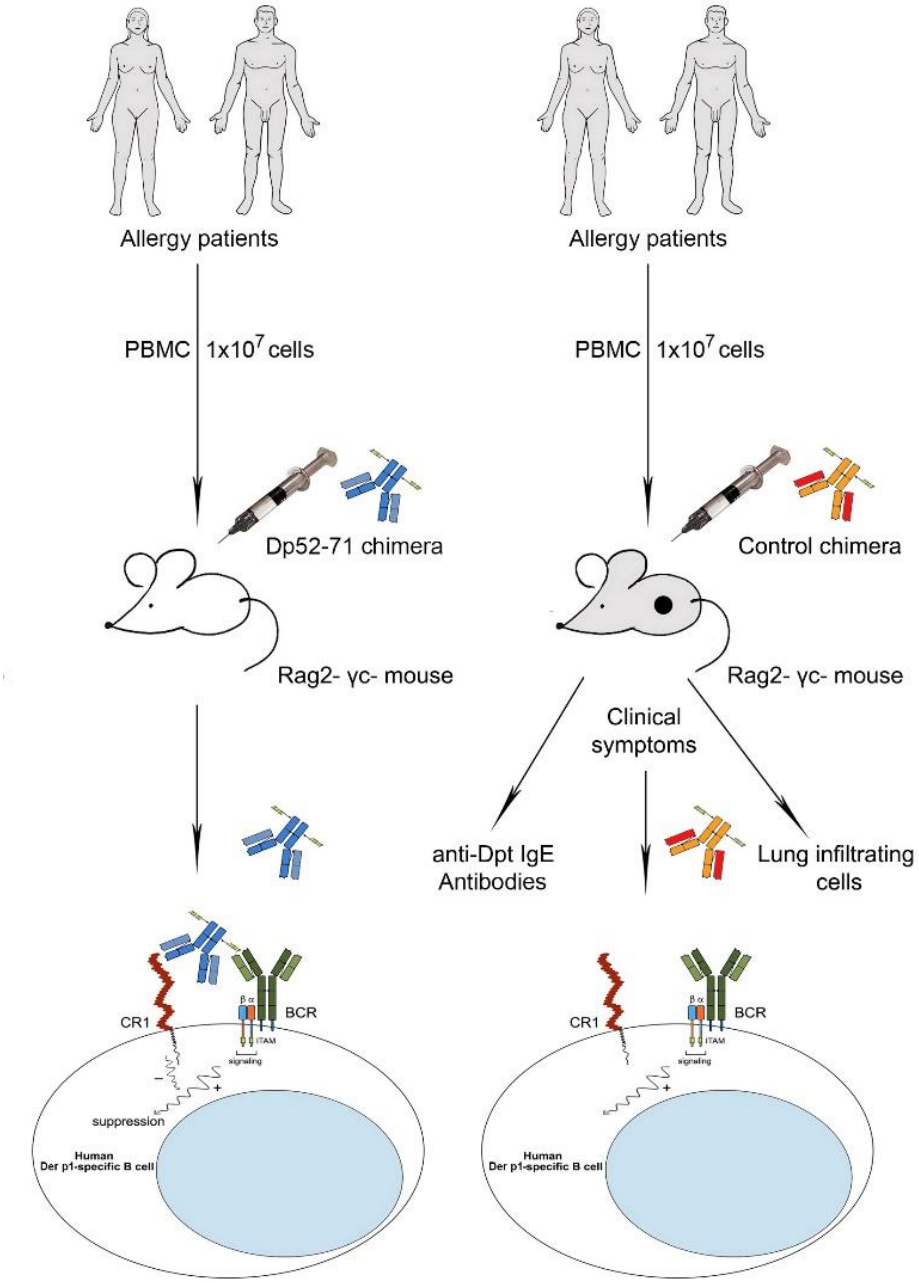


**Figure 1.** Schematic representation of PBMC transfer from HDM-allergic patients into Rag2- γc- mice and experimental therapeutic design.

A detailed treatment scheme is presented in Figure 2. On day 30 post-transfer, a bronchoalveolar lavage (BAL) was performed via the trachea. Bronchoalveolar lavage fluid (BALF) were collected by washing with 1 ml of ice-cold PBS, followed by centrifugation at 600 × g at 4°C. The supernatants were then stored at -80°C for further analysis.

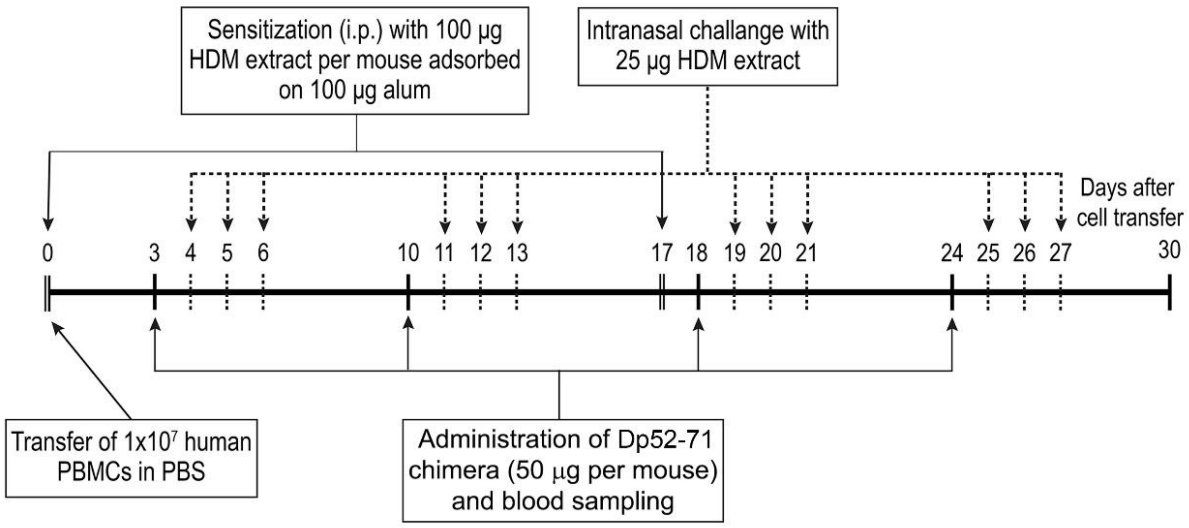


**Figure 2.** Development of the humanized Rag2- γc- model of HDM allergy and treatment scheme with chimeric protein molecules.

### 1.6. Analysis of Anti-Dpt IgE, IgA, IgG, and Total IgE Antibodies

The levels of anti-Dpt IgE antibodies in BALF were determined using a highly sensitive fluorescent enzyme-linked immunosorbent assay (ELISA). Opaque 96-well flat-bottom plates (Cat# 675076, Greiner Bio-One, Kremsmünster, Austria) were coated with 100 µg/mL of Dpt extract diluted in 50 mM carbonate buffer (pH 9.6) and incubated overnight at 4 °C. Plates were blocked with 1% bovine serum albumin (BSA) in 0.05% Tween 20 in PBS (T-PBS) for 2 hours at room temperature (RT) and then incubated with BALF for 2 hours at RT. Following this, the plates were washed and incubated for an additional 2 hours with biotin-conjugated anti-human IgE antibody (1:1000 dilution) (Cat# 16-10-04, Kirkegaard & Perry Laboratories, Gaithersburg, Maryland, US), followed by incubation with HRP-conjugated streptavidin (1:1000 dilution) (Cat# S5512, Sigma-Aldrich) for 40 minutes at RT. The reaction was developed using a highly sensitive ADHP (10-acetyl-3, 7-dihydroxyphenoxazine) SensoLyte Peroxidase Substrate (Cat# AS-71111, Anaspec, Fremont, CA). The resulting fluorescent product was analyzed using an automated fluorescence reader (BMG Labtech, Offenburg, Germany) with an excitation wavelength of 530 nm and detection at 590 nm.

The levels of anti-Dpt IgA and anti-Dpt IgG antibodies in BALF were determined using ELISA, following the same antigen-coating and blocking procedure described above. After 2 hours of incubation with BALF samples, plates were incubated with anti-human IgA (1:1000 dilution) (Cat# 2050-04, Southern Biotech, Birmingham, AL) or IgG (1:10000 dilution) (Cat# A-1543, Sigma-Aldrich) antibodies conjugated to alkaline phosphatase. The reaction was

developed using 1 mg/mL pNPP (p-Nitrophenyl Phosphate, Disodium Salt) substrate (Cat# 4876, Calbiochem, San Diego, CA) and measured at 405 nm.

The total human IgE levels in BALF were measured using an ELISA kit for IgE (Cat# EV 3840-9601 E, Euroimmun, Lübeck, Germany), following the manufacturer's protocol. Briefly, pre-coated wells with anti-human IgE antibodies were incubated with 100 µL of samples per well for 30 minutes at RT. After three washes, the wells were incubated with 100 µL of anti-human IgE antibody conjugated with horseradish peroxidase for 30 minutes at RT. Following three washes, the wells were incubated with substrate for 15 minutes at RT, protected from light. The reaction was stopped, and absorbance was measured at 450 nm with a reference wavelength of 620 nm.

For all ELISA analyses, each incubation step was followed by at least three washing steps using 200 µL/well of T-PBS.

### 1.7. Investigation of β-hexosaminidase activity and total protein concentration in BALF

The activity of β-hexosaminidase in BALF was investigated as a marker for mast cell degranulation in the lungs. The enzyme reaction was initiated by mixing 50 µl of BALF and 50 µl of 5 mM p-nitrophenyl N-acetyl-β-d-glucosaminide (Cat# 4062.2, Carl Roth, Karlsruhe, Germany) dissolved in a buffer containing 50 mM trisodium citrate, pH 4.5 (Cat# S1804, Sigma-Aldrich). After incubation for 2 hours at 37 °C, the reaction was stopped by adding 200 µl of 0.2 M glycine-NaOH (pH 10.6), (Cat# 15527, Riedel-de-Haën; Cat# S5881, Sigma-Aldrich). The optical density was measured at 405 nm.

The total protein concentration in BALF was measured using Bradford reagent (Cat# B6916, Sigma-Aldrich) according to the manufacturer's protocol. Briefly, BALF samples were mixed with Bradford reagent in a 1:30 ratio at a final volume of 200 µl/well in a 96-well plate. The absorbance was measured at 595 nm. Serial dilutions of BSA (1.4 mg/ml to 0.0625 mg/ml) were used to determine the protein concentration.

### 1.8. Phenotyping of lung infiltrates

The right lung lobes of the humanized Rag2- γc- mice were analyzed for the presence of human lymphocyte populations using FACS analysis. Cells were isolated from the lungs using a buffer containing 2 mg/ml collagenase D (Cat# 11088858001, Sigma-Aldrich) and 0.1 mg/ml DNase I (Cat# 10104159001, Sigma-Aldrich) at 37°C for 45 minutes. A single-cell suspension was then obtained by passing the lung tissue through a 70 µm cell strainer. Viable cells were counted using a Bürker chamber, and 2 × 10^5 cells/test tube were allocated for FACS analysis. After

two centrifugation steps with 1 ml/tube of FACS buffer (2.5% fetal bovine serum in PBS) for 10 minutes at 1200 rpm at 4°C, lymphocytes were incubated with an antibody cocktail for phenotyping. Human lymphocytes were identified by anti-human CD45-FITC antibody, and T-cells were identified by labeling with anti-human CD3-PeCy7, CD4-APC, and CD8a-PE antibodies. B-cells were identified with anti-human CD19-eFlour450 antibody. Thirty thousand CD45-positive cells from each sample were analyzed using a BD LSR II flow cytometer with Diva 6.1.1. software (BD Biosciences, San Jose, California).

### 1.9. Histopathological analysis of lungs

The left lobe of the lungs from each humanized Rag2- γc- mouse was dissected and fixed in 10% formalin (Cat# HT501128, Sigma-Aldrich) overnight. The fixed lungs were dehydrated in increasing concentrations of ethanol (70%, 80%, 95%, and 100%) and xylene substitute (Cat# 1426, Tissue-clear, Sakura Finetek Europe), followed by embedding in paraffin (Cat# P3558, Paraplast, Sigma-Aldrich). Paraffin sections of 5 μm thickness were analyzed using the standard hematoxylin and eosin (H&E) staining technique (Cat# GHS216; Cat# HT110, Sigma-Aldrich). Microscope slides were observed using a light microscope (40×, Nikon Eclipse E100, Melville, NY). Perivascular and peribronchial inflammation were assessed (histological inflammatory score) using ImageJ software. The data were calculated using the formula: *area of cellular infiltrates around vessels / area of vessels*.

### 1.10. Statistical analysis

All statistical analyses were performed using GraphPad Prism 5 software (San Diego, California). An unpaired t-test or paired t-test was used to determine the differences between groups. Data are presented as the mean ± SD. A p-value of $<0.05$ was considered statistically significant.

## 2. Chronic mouse model of house dust mite allergy

### 2.1. Antibodies

The hybridoma cell line 2.4G2, producing monoclonal IgG2b antibody specific for mouse FcγRII (CD32) (ATCC HB-197), was cultured in serum-free RPMI medium (Gibco, Gaithersburg, MD). The antibodies were isolated and purified from the supernatant [167]. Fluorescein isothiocyanate (FITC)-conjugated anti-mouse CD16/32 antibody (Cat# 35-0161-U100, clone 2.4G2, Tonbo Bioscience, San Diego, CA), anti-mouse IgG-FITC antibody (Cat# 405404, BioLegend, San Diego, CA), anti-mouse FITC-conjugated CD11c (Cat# 117306, clone N418, BioLegend), CD25 (Cat# 102006, clone PC61, BioLegend), CD45R (B220) (Cat#

103206, clone RA3-6B2, BioLegend); Phycoerythrin (PE)-conjugated CD19 (Cat# 115508, clone 6D5, BioLegend), SiglecF (Cat# 12-1702-80, clone 1RNM44N, eBioscience, Frankfurt, Germany), CD69 (Cat# 104508, clone H1.2F3, BioLegend), and CD138 (Cat# FAB2966P, clone 300506, R&D Systems, Minneapolis, MN); PE-Cyanine 7 (PE-Cy7)-conjugated CD3 (Cat# 100320, clone 145-2C11, BioLegend) and CD8 (Cat# 100722, clone 53-6.7, BioLegend); Pacific Blue-conjugated Ly6G (Cat# 127612, clone 1A8, BioLegend), CD3 (Cat# 100334, clone 145-2C11, BioLegend), and CD80 (Cat# 104724, clone 16-10A1, BioLegend); PE-Cyanine 5 (PE-Cy5)-conjugated CD4 (Cat# 100410, clone GK1.5, BioLegend) and streptavidin (Cat# 15-4317-82, eBioscience); biotin-conjugated IgE (Cat# 13-5992-85, clone 23G3, eBioscience) monoclonal antibodies were used for the FACS analysis experiments. Corresponding isotype control IgG antibodies were used for compensation and validation of antibody signals. Horseradish peroxidase (HRP)-conjugated anti-mouse IgG (Cat# 405306, BioLegend), biotin-conjugated anti-mouse IgG1 (Cat# 406604, clone RMG1-1, BioLegend), IgM (Cat# 406504, clone RMM-1, BioLegend) and IgA antibodies (Cat# 407004, clone RMA-1, BioLegend), and streptavidin-conjugated HRP (Cat# S5512, Sigma-Aldrich, Taufkirchen, Germany) were used in ELISA analyses.

### 2.2. Construction of Protein-Engineered Chimeric Molecules

Two synthetic peptides and the monoclonal antibody 2.4G2, specific for murine CD32, were used to construct chimeric molecules through protein engineering. Selected epitope-bearing peptides p52-71 from Der p 1 (Ac-NQSLDLAEQELVDCASQHGC-Ahx-K-$NH_2$) and control (irrelevant) peptides (Ac-DEACLQCGSEDHQAVQNLLS-Ahx-K-$NH_2$), containing the same amino acids in a random order, were purchased from Caslo Laboratory (Lyngby, Denmark). During peptide synthesis via an Fmoc-based solid-phase reaction with >96% purity, an Ahx linker with lysine was introduced at the C-terminus of the peptides. The Dp52-71 chimera was constructed by conjugating the 2.4G2 antibody to Der p 1 peptides. An irrelevant (control) chimera, consisting of the same antibody conjugated to control peptides, was also generated.

Chemical conjugation in protein engineering was performed as previously described [175]. Briefly, a classical EDC (1-ethyl-3(3’-dimethylaminopropyl) carbodiimide.HCl) (Cat# E6383, Sigma-Aldrich) cross-linking technique was applied to conjugate the peptides at a 20-fold molar excess relative to the 2.4G2 antibody and a 60-fold molar excess of the zero-length crosslinker carbodiimide. The reaction took place in phosphate conjugation buffer (pH 6.0) overnight (ON) at 4°C. The reaction mixture was then purified from unconjugated peptides by

three rounds of dialysis on a magnetic stirrer against PBS at a PBS:reaction mixture ratio of 50:1, ON at 4°C, followed by two additional rounds of dialysis for two hours at RT. The chimeric molecules were then concentrated by ultrafiltration (Amicon XM50 membrane) and sterilized through a 0.20 µm filter. The concentration of the chimeric molecules was measured at 280 nm.

### 2.3. Characterization of Chimeric Molecules

#### 2.3.1. Examination of the Binding of Chimeric Molecules to FcγRIIb via FACS Analysis

The spleens of healthy mice and HDM-allergic mice were dissected, and single-cell suspensions were obtained by filtering through a 70 µm cell strainer. After lysing erythrocytes in a hypotonic buffer, the cells were washed in PBS, counted using a Bürker chamber, and distributed into FACS tubes ($2 \times 10^5$ cells/tube). The cells were then washed twice with 1 ml/tube of FACS buffer (2.5% FBS/PBS) at 1200 rpm, 4°C, and subsequently used for further analyses.

The binding of chimeric molecules to B and T cells was investigated using the following protocol: cells were incubated on ice for 20 minutes with 2.4G2 antibody, Dp52-71 chimera, or irrelevant chimera (0.8 µg/tube) and then washed. Anti-rat IgG-FITC antibody was then applied under the same conditions to detect the rat-derived 2.4G2 antibody and chimeras. After washing, the cells were incubated with CD3-PE-Cy7 and CD19-PE antibodies.

To assess whether the chimeras bind to FcγRIIb, a competitive FACS analysis was performed. Splenocytes were incubated on ice for 20 minutes with serial two-fold dilutions of the 2.4G2 antibody, Dp52-71 chimera, or irrelevant chimera (0.2, 0.4, 0.8, 1.6 µg/tube). After washing, anti-CD16/CD32 (2.4G2)-FITC, CD3-PE-Cy7, and CD19-PE antibodies were added.

Thirty thousand cells within the lymphocyte population were analyzed using a BD LSR II flow cytometer (BD Biosciences, Mountain View, CA) and FlowJo software (Ashland, OR).

#### 2.3.2. Recognition of Chimeric Molecules by Serum IgG1 Antibodies

Dp52-71 or irrelevant chimera (100 µl/well, 10 µg/ml), diluted in coating buffer (0.015 M $Na_2CO_3$, 0.035 M $NaHCO_3$, pH 9.6), was incubated in a 96-well plate overnight at 4°C. The wells were blocked with 200 µl of 1% BSA in T-PBS for 2 hours at room temperature (RT). The plates were then incubated with three-fold serial dilutions (10x, 30x, 90x, 270x) of sera from healthy BALB/c mice and from animals subcutaneously injected four times (days 0, 21,

35, 49) with 100 µg/mouse HDM extract adsorbed onto 100 µg $Al(OH)_3$ (Alum) for 2 hours at RT.

Next, a biotin-conjugated anti-mouse IgG1 antibody (diluted 1000x) was added for a 1-hour incubation at RT, followed by incubation with streptavidin-HRP (diluted 500x) under the same conditions. After extensive washing, the enzymatic reaction was developed using 0.1 mg/ml 3,3',5,5'-tetramethylbenzidine (TMB) substrate (100 µl/well, Cat# 87748, Sigma-Aldrich) in 0.05 M phosphate-citrate buffer (pH 5.0) and 1.96 mM $H_2O_2$. The reaction was stopped by adding 2 N $H_2SO_4$ (50 µl/well) and measured at 450 nm with correction at 570 nm (CLARIOstar Plus, BMG LABTECH).

### 2.4. BALB/c Mice

Female BALB/c mice, 8 weeks old, were purchased from The Jackson Laboratory (Bar Harbor, ME) and housed under SPF conditions in the animal house facility of the Institute of Microbiology, strictly following the guidelines of EU Directive 2010/63/EU and in compliance with national regulations.

### 2.5. Generation of a Chronic Mouse Model of HDM Allergy and Treatment Scheme

BALB/c mice were randomly divided into four groups (9 animals per group). The mice were anesthetized, and 25 µg of HDM extract in 35 µl PBS was administered intranasally (i.n.) to three of the groups. Sensitization with HDM extract was performed twice per week (with a one-day interval between treatments) for two weeks (days 0, 2, 7, and 9), followed by five additional i.n. challenges once per week (days 14, 22, 29, 36, and 43). During the last four weeks, mice were injected intravenously once per week with 50 µg of Dp52-71 chimera, irrelevant chimera, or PBS in a volume of 100 µl, one day before i.n. HDM challenge (days 21, 28, 35, 42). The control group (PBS group) received i.n. and i.v. PBS following the same schedule. The mice were bled via the retro-orbital sinus 24 hours after the final HDM challenge, and collected sera were stored at -80°C. The animals were sacrificed, and BAL, lungs, and spleens were isolated.

### 2.6. Isolation of BALF and Differential Cell Counting

Three volumes of 1 ml ice-cold PBS were introduced through the trachea into the lungs of each mouse, and the volume of the recovered fluid was measured. The samples were centrifuged for 10 minutes at 600 × g, 4 ºC, and the supernatant from the first injection volume was collected and stored at -80 ºC for subsequent BALF analysis. The cell pellets from the three lung lavages

of each mouse were pooled and centrifuged under the same conditions. Then, erythrocytes were lysed with 200 µl of hypotonic buffer, followed by centrifugation. The pellets were resuspended in 500 µl PBS, and the cells were counted using a hemocytometer. Fifty thousand cells were placed onto glass slides for cytospin and centrifuged for 10 minutes at 700 rpm. The slides were air-dried and stained using the Differential Quik Stain Kit (Cat# 24606, Polysciences, Niles, IL) according to the manufacturer's instructions. The cells were observed under a microscope (200× magnification, Leica DM2000, Leica Microsystems). Six visual fields per slide were analyzed using ImageJ software (200–400 cells per mouse). Finally, the results were calculated as the number of cells per milliliter of recovered fluid and as percentages.

### 2.7. Detection of anti-HDM IgG, IgG1, IgM, and IgA in serum and BALF

HDM extract (10 µg/ml in coating buffer, pH 9.6) was incubated in 96-well plates (50 µl/well) overnight at 4 ºC. The wells were washed with T-PBS and blocked with 200 µl/well of 1% BSA in T-PBS for 2 hours at RT. Then, 50× diluted mouse sera or 3× diluted BALF samples in 1% BSA in T-PBS (50 µl per well) were added and incubated for 2 hours at RT. After washing, the plates were incubated with 2000× diluted HRP-conjugated anti-mouse IgG antibody (50 µl/well) or with 1000× diluted biotin-conjugated anti-mouse IgG1, IgM, or IgA antibodies for 1 hour at RT. Samples with biotin conjugates were further incubated for 1 hour with 500× diluted streptavidin-HRP. The enzymatic reaction was developed by adding TMB substrate, as described above, and measured.

### 2.8. Investigation of total IgE antibodies, IL-4, IL-5, IL-9, and IL-13

The concentration of total IgE antibodies was measured in BALF samples (10× diluted) and serum samples (800× diluted) using the ELISA MAX™ Deluxe Set, following the manufacturer's instructions (Cat# 432404, BioLegend).

The concentrations of IL-4 (Cat# 431104, BioLegend), IL-5 (Cat# 431204, BioLegend), IL-9 (Cat# 88-8092, Invitrogen), and IL-13 (Cat# 88-7137, Invitrogen, Waltham, MA) in BALF were determined according to the manufacturer's protocol with minor modifications. The volumes of primary antibody, BALF samples (2.15× diluted), detection antibody, and enzyme substrate were adjusted to 50 µl/well.

Briefly, the detection procedure for total IgE antibodies, IL-4, and IL-5 involved the following steps. Antibodies specific for mouse IgE, IL-4, or IL-5 were incubated for 16-18 hours at 4 ºC in 96-well plates. The plates were then washed four times with 300 µl/well Wash Buffer, and

non-specific binding was blocked with 200 µl/well Assay Diluent A for 1 hour at room temperature (RT). After washing as described above, diluted BALF or serum samples in Assay Diluent A were added and incubated for 2 hours at RT. Following another wash, the plates were incubated with Detection Antibody for 1 hour at RT. After washing, the plates were incubated with Avidin-HRP for 30 minutes at RT. Following thorough washing, the plates were incubated with TMB Substrate in the dark for 20 minutes, after which the enzymatic reaction was stopped with Stop Solution, and absorbance was measured at 450 nm with signal correction at 570 nm. The concentration of the analyzed proteins was calculated using a standard curve.

For IL-9 and IL-13 cytokine analysis, the following protocol was used. Anti-IL-9 and anti-IL-13 antibodies were incubated in a 96-well plate at 4 ºC overnight. The plates were washed three times with 250 µl/well Wash Buffer and blocked with 200 µl/well 1X ELISA/ELISPOT Diluent for 1 hour at RT. After a single wash, wells were incubated with BALF samples diluted in 1X ELISA/ELISPOT Diluent for 2 hours at RT. The plates were washed five times and incubated with Detection Antibody diluted in 1X ELISA/ELISPOT Diluent for 1 hour at RT. After five additional washes, Avidin-HRP was added for 30 minutes at RT. The plates were washed seven times, followed by incubation with 1X TMB Substrate for 15 minutes at RT. The reaction was stopped with Stop Solution, and absorbance was measured at 450 nm with signal correction at 570 nm. The concentration of the analyzed cytokines was calculated using a standard cytokine curve.

### 2.9. Investigation of total protein concentration and β-hexosaminidase activity in BALF

The enzymatic activity of β-hexosaminidase and the total protein concentration in BALF samples were measured as described in Section III.1.7.

### 2.10. Phenotyping of pulmonary cellular infiltrates

The right lung lobes were cut into small pieces and incubated in a buffer containing 0.1 mg/ml DNase I (Cat# 10104159001, Sigma-Aldrich) and 2 mg/ml collagenase D (Cat# 11088858001, Sigma-Aldrich) for 45 minutes at 37 °C. A single-cell suspension was obtained by filtering the dissociated homogenized lungs through a 70 µm cell strainer. The isolated cells were centrifuged for 10 minutes at 1200 rpm, 4 °C, followed by red blood cell lysis using a hypotonic buffer. The cells were then centrifuged again, counted, distributed into FACS tubes ($2 \times 10^5$ cells per tube), and washed twice with FACS buffer.

Phenotyping of immune cells was performed by incubation with the following four panels of anti-mouse antibodies for 20 minutes on ice: Myeloid cells: Ly6G-Pacific Blue, CD11c-FITC, SiglecF-PE; B cells: CD19-PE, CD80-Pacific Blue, CD16/CD32-FITC, IgE-biotin, followed by a secondary incubation with Streptavidin-PE-Cy5; Antibody-secreting cells: CD138-PE, CD45R (B220)-FITC; T cells: CD3-Pacific Blue, CD4-PE-Cy5, CD8-PE-Cy7, CD25-FITC, CD69-PE.

The tubes were then washed twice, and 30,000 cells per sample were analyzed using a BD LSR II flow cytometer. The collected data were exported using DIVA software and analyzed with FlowJo software.

### 2.11. Histology

The left lung lobes from each mouse were fixed in 10% neutral buffered formalin (Cat# 3800598, Leica Biosystems). The fixed tissue was processed using an automated tissue processor (Leica TP1020, Leica Biosystems) through increasing concentrations of ethanol (30 minutes in 70%, 80%, 95%, and twice for 30 minutes in 100%) and Waxsol Cleaning Solution (twice for 45 minutes) (Cat# S26.0390, Leica Biosystems). The lungs were then embedded (Leica HistoCore Arcadia H and C, Leica Biosystems) in paraffin (Cat# P3558, Paraplast, Sigma-Aldrich) and sectioned into 5 μm slices (Leica RM2125 RTS, Leica Biosystems).

The paraffin sections were deparaffinized in Waxsol Cleaning Solution (10 minutes) and decreasing concentrations of ethanol (6 minutes in 100%, 3 minutes in 95%, 1 minute in 80% and 70%), followed by staining with hematoxylin and eosin (H&E) (Cat# 1.05175; Cat# 1.09844, Sigma-Aldrich) and Periodic Acid-Schiff (PAS) (Cat# PAS5-K-100, Biognost).

Hematoxylin and Eosin (H&E) staining was performed according to the following protocol. The deparaffinized lung sections were hydrated in distilled water for 2 minutes. The slides were stained with Hematoxylin Solution, Gill.2, for 3 minutes, followed by three washes with tap water. The sections were then stained with an acidified solution of Eosin Y for 1 minute and rinsed once with tap water. Finally, the sections were dehydrated through increasing concentrations of ethanol (1 minute in 70% and 80%, 2 minutes in 95%, and 6 minutes in 100%) and Waxsol Cleaning Solution (5 minutes), followed by coverslipping.

PAS staining was performed according to the following protocol. The deparaffinized lung sections were hydrated in distilled water for 2 minutes. The sections were then incubated with a 0.8% periodic acid solution for 10 minutes, followed by rinsing with tap water for 3 minutes and immersion in distilled water. Lung sections were incubated with BioSchiff reagent for 15 minutes, followed by incubation with sulfite solution for 6 minutes. The samples were washed

with tap water for 3 minutes, then counterstained with Hematoxylin ML for 3 minutes. Finally, the sections were washed for 3 minutes with tap water, immersed in distilled water, dehydrated, and coverslipped.

Slides were examined and imaged using a Leica DM2000 microscope (Leica Microsystems) at 200X magnification. Perivascular and peribronchial inflammation was assessed (histological inflammatory score) using ImageJ software. Data were calculated using the formula: perivascular infiltrate area / vessel area [176]. A five-point scoring system was used for the PAS score: 0, <0.5% PAS-positive cells; 1, <25%; 2, 25–50%; 3, 50–75%; and 4, >75% [177]. Six to thirteen bronchioles per mouse were analyzed.

### 2.12. Statistical analysis

Most statistical analyses were performed using GraphPad Prism 9. Data are presented as mean ± SD, with a p-value $< 0.05$ considered statistically significant. ELISA and cytokine assays were conducted in duplicate. Normality of data distribution was assessed using the Shapiro-Wilk and Kolmogorov-Smirnov tests.

Depending on the normality of the data distribution, statistical significance was evaluated using one-way or two-way ANOVA tests, followed by Tukey's multiple comparisons test, or the Kruskal-Wallis test followed by Dunn's multiple comparisons test. Correlation analyses were conducted using Spearman and Pearson tests. The Spearman correlation matrix was generated using the SRplot software available at bioinformatics.com.cn [178].

# IV. RESULTS

## 1. Humanized Mouse Model of House Dust Mite Allergy

### 1.1. Treatment with Human Dp52-71 Chimera Reduces Anti-Dpt IgE Levels, Total Protein, and β-Hexosaminidase Activity in BALF

PBMCs isolated from untreated allergic patients diagnosed with Dpt sensitivity and high levels of anti-Dpt IgE antibodies were transferred into female Rag2- γc- mice. The humanized Rag2-γc- mice were treated with Dp52-71 or the control chimera to assess the *in vivo* effect of Dpt-specific B-cell suppression (Figures 1 and 2). The animals were weighed and monitored throughout the experiment, and no signs of graft-versus-host reaction were observed (data not shown).

BAL supernatants were analyzed to determine the local immune response in the humanized HDM allergy model, as additional allergen stimulation was performed intranasally. Since increased levels of anti-Dpt IgE antibodies are a hallmark of HDM allergy, we measured the levels of allergen-specific IgE in the BALF of treated animals. The results showed that therapy with the Dp52-71 chimera significantly reduced human anti-Dpt IgE antibody levels compared to the control chimera (Figure 3A). However, no changes were observed in the levels of allergen-specific IgA, IgG, or total IgE antibodies (Figures 3B–D).

Total protein concentration in BALF is used as a marker of vascular permeability in the lungs. Treatment with the Dp52-71 chimera led to a reduction in protein levels in the BALF exudate (Figure 3E). Mast cell degranulation in the lungs was assessed by measuring β-hexosaminidase enzyme activity in BALF. The release of β-hexosaminidase into the airways was significantly inhibited in the group injected with the Dp52-71 chimera (Figure 3F).

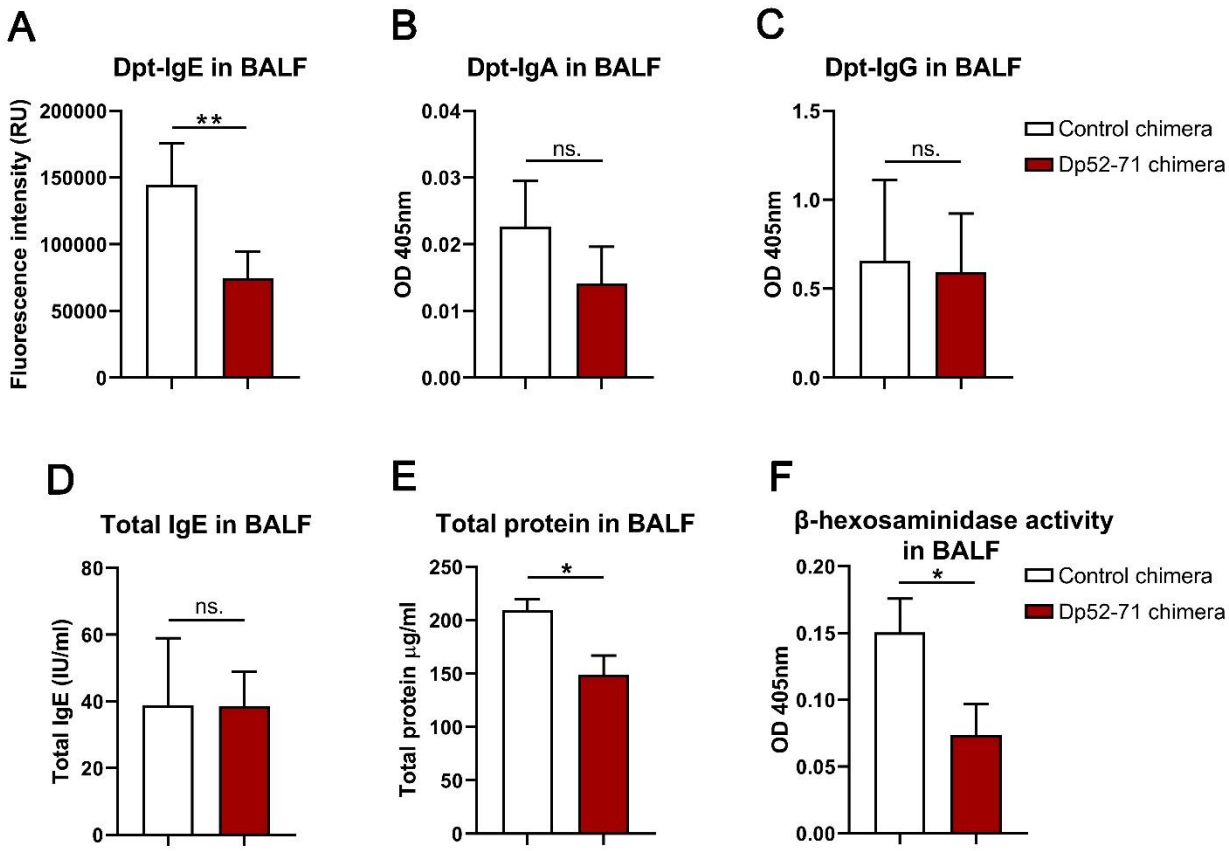


**Figure 3.** Analysis of BALF Samples. PBMCs from each HDM allergy patient (n = 4) were injected into two Rag2- γc- mice, followed by treatment of the experimental animals with either the control chimera or Dp52-71 chimera. Each sample represents BALF from an individual animal. (A) Anti-Dpt IgE levels in BALF were measured by fluorescent ELISA. Anti-Dpt IgA (B) and anti-Dpt IgG (C) levels in BALF were measured by ELISA. Total IgE antibody concentration (D) and total protein concentration (E) in BALF were evaluated. β-Hexosaminidase activity in BALF was measured and used as an indication of mast cell degranulation (F). Data are presented as mean ± SEM from 4 mice per group; p-values were calculated using paired t-tests to determine differences between the Dp52-71 chimera-treated group (*$p<0.05$; **$p<0.01$) compared to mice injected with the control chimera.

### 1.2. Effect of human Dp52-71 chimera on human lymphocyte infiltration in lungs of humanized mice

Lymphocyte infiltration in the lungs of humanized mice was examined through FACS analysis of cell suspensions isolated from the right lobes of the lungs of all animals (Figure 4).

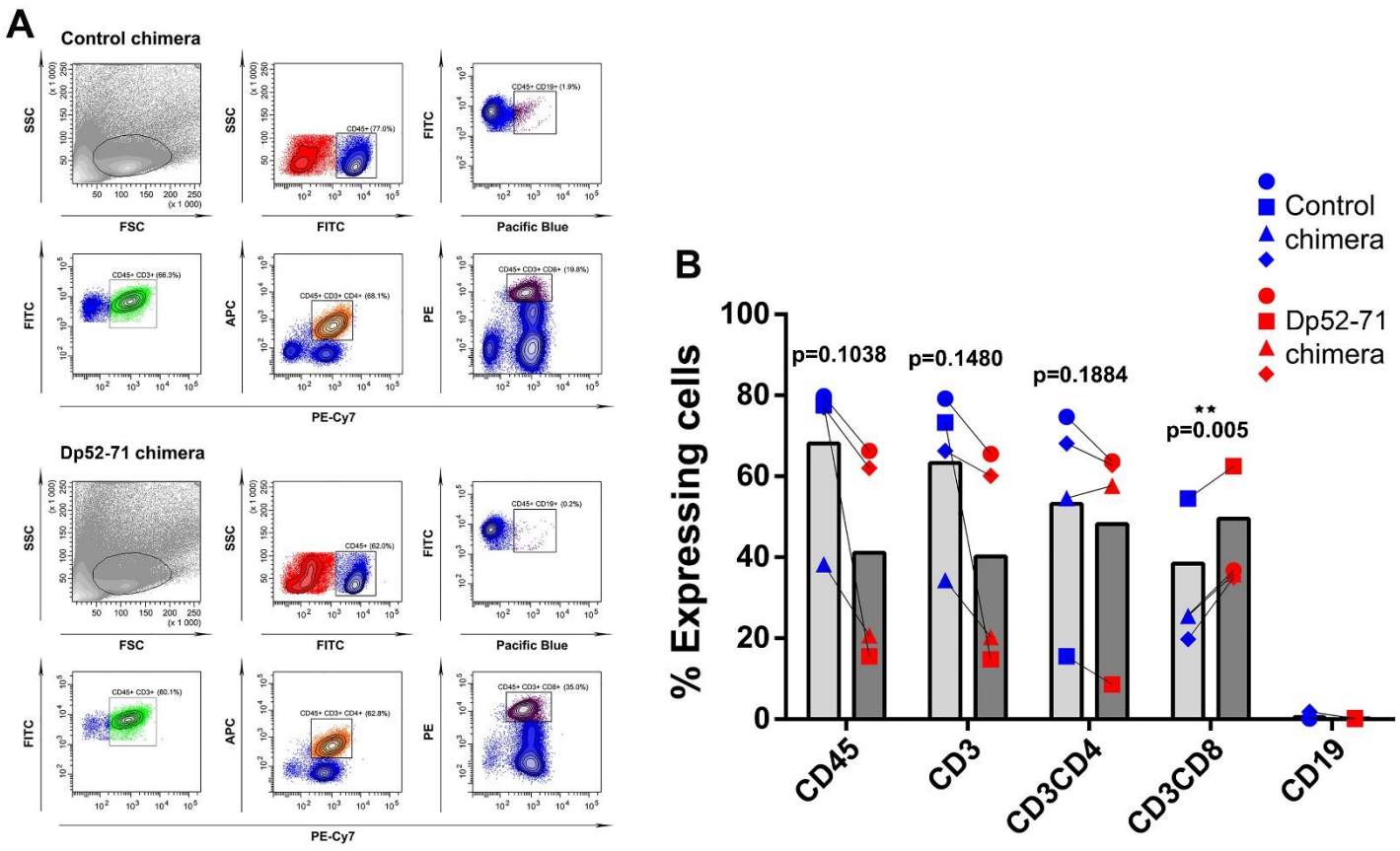


**Figure 4.** Phenotyping of pulmonary infiltrates. (A) Single-cell suspensions were isolated from the lungs of all animals, then analyzed using the following combinations of anti-human antibodies along with CD45-FITC: CD3-PeCy7, CD3-PeCy7/CD4-APC, CD3-PeCy7/CD8a-PE, or CD19-eFluor450. Thirty thousand CD45-positive cells from each sample were analyzed using flow cytometry. (B) The resulting data are presented graphically as the percentage of total immune cells. Each symbol (circle, square, triangle, and diamond) represents cells from an individual animal transferred with cells from a patient with HDM allergy (n = 4), treated with control chimera (blue) or Dp52-71 chimera (red). The data are presented as values from 4 mice per group; p-values were calculated using a paired t-test to determine differences between the Dp52-71 chimera-treated group (**p<0.01) compared to mice injected with control chimera.

A trend of reduced numbers of human CD45, CD3, and CD4 cells was observed in the group treated with Dp52-71 chimera compared to the animals treated with the control chimera. A statistically significant increase in the percentage of infiltrating CD8 T cells was observed in the Dp52-71 chimera-treated group compared to the control group of mice. A small percentage of B cell infiltration in the lungs was observed in some of the humanized animals (Figure 4B).

### 1.3. Treatment with the human Dp52-71 chimera reduces overall lung inflammation

At the end of the *in vivo* experiments, the left lung lobes from all animals were used for histopathological analysis through hematoxylin and eosin staining. As illustrated in Figure 5, perivascular and peribronchial inflammatory cell infiltrates were observed in the lungs of mice treated with the control chimera and humanized with PBMCs from allergic patients following intranasal stimulation with HDM. In contrast, no such severe pathological inflammation was found in the lungs of the Dp52-71 chimera-treated humanized mice, with a statistically significant reduction in perivascular cell infiltrates being observed.

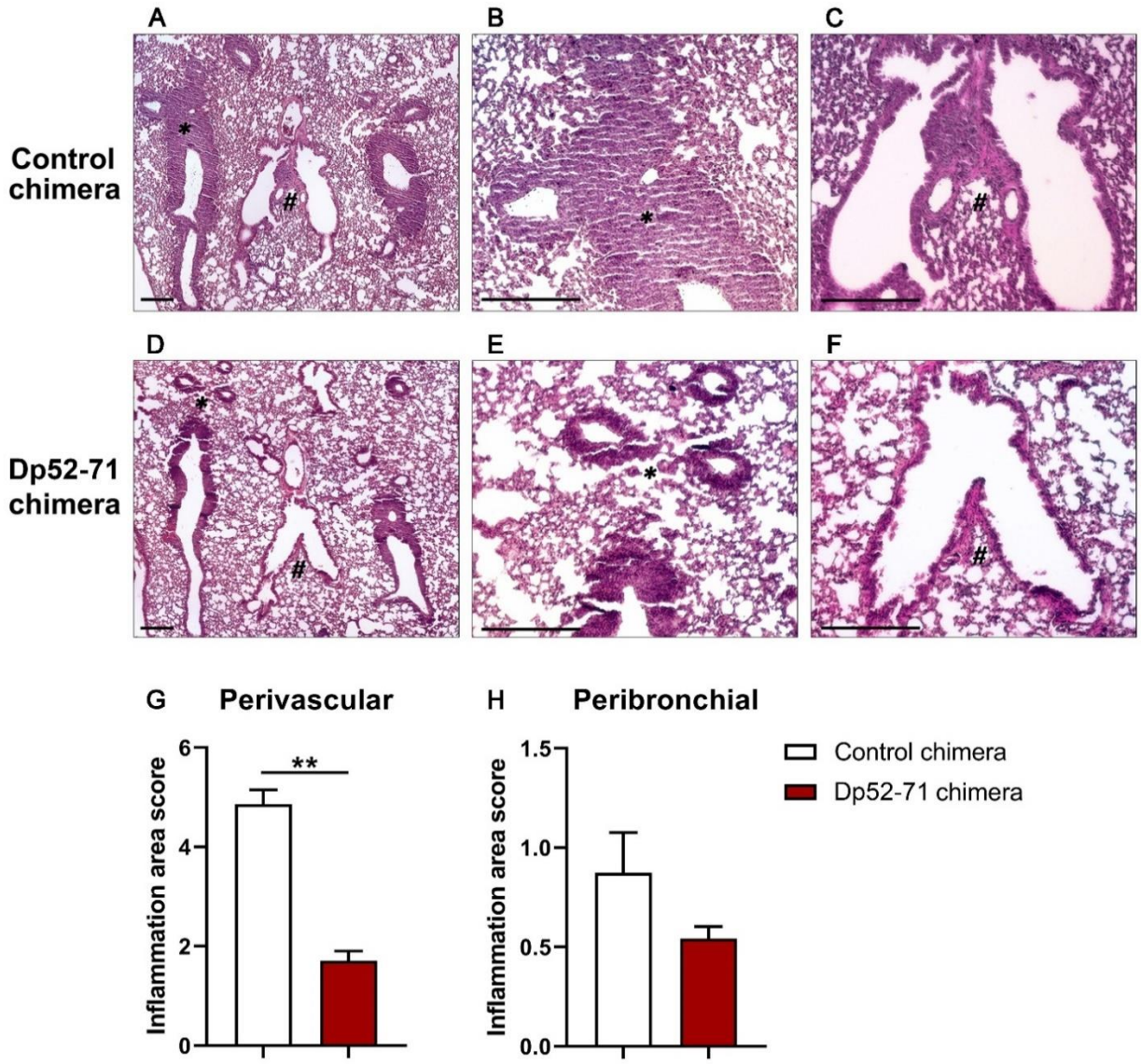


**Figure 5.** Histology of lungs from humanized Rag2- γc- mice. Histological examination of paraffin sections of lungs from Rag2- γc- mice, humanized with PBMCs from HDM allergy patients and treated with control chimera (A–C) or Dp52-71 chimera (D–F). Perivascular (*) and peribronchial (#) inflammatory infiltrates were found in the lungs of humanized mice following intranasal stimulation with HDM (25 µg/mouse). Standard hematoxylin and eosin staining technique was used. Representative images from 4 animals are shown. Scale bar, 250 µm. Histological evaluation (histological inflammatory score) of perivascular (G) and peribronchial (H) inflammation. Data are presented as mean ± SD; p-values were calculated using a paired t-test to determine differences between the Dp52-71 chimera-treated group (**p<0.01) compared to mice injected with the control chimera.

## 2. Chronic mouse model of house dust mite allergy

### 2.1. Characterization of chimeric molecules

Dp52-71 and irrelevant chimera were constructed by conjugating the mouse monoclonal antibody 2.4G2 with peptide epitopes from the allergen Der p 1, or with irrelevant peptides, respectively. The ability of the chimeric molecules to bind to the FcγRIIb receptor was assessed through FACS analysis using splenocytes from healthy and HDM-treated mice (Figure 6).

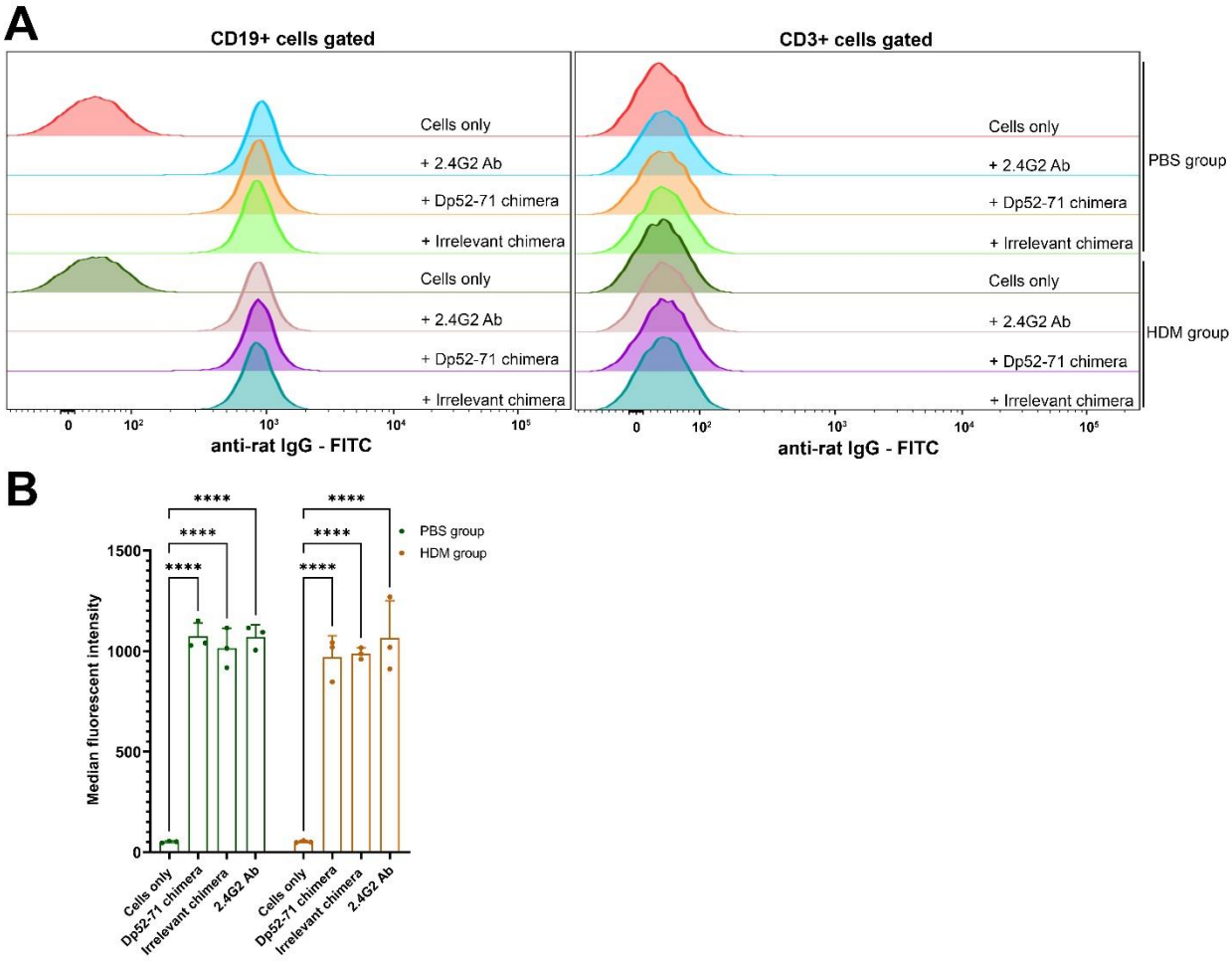


**Figure 6.** The Dp52-71 chimera recognizes the FcγRIIb receptor on mouse B cells. (A) The binding of Dp52-71 and irrelevant chimera to the surface of CD19 and CD3 cells was determined through FACS analysis. Splenocytes from healthy and HDM-stimulated mice were incubated with the chimeras or 2.4G2 antibody, followed by incubation with FITC-conjugated anti-mouse IgG antibody. (B) A summary graph presenting the median fluorescence intensity of the FITC-conjugated anti-mouse antibody. Data are presented as mean ± SD from at least 3 mice per group. Differences between groups were assessed by two-way ANOVA followed by Tukey's multiple comparisons test; ****p<0.0001.

Dp52-71 and irrelevant chimera bind to the surface of CD19 cells with the same intensity as the pure 2.4G2 antibody in both PBS and HDM-stimulated mice (Figure 6A left, B). No similar binding was observed in the CD3-positive cell population (Figure 6A right).

We further analyzed the ability of the chimeric molecules to compete with commercially available FITC-conjugated 2.4G2 antibody for binding to the FcγRIIb receptor (Figure 7).

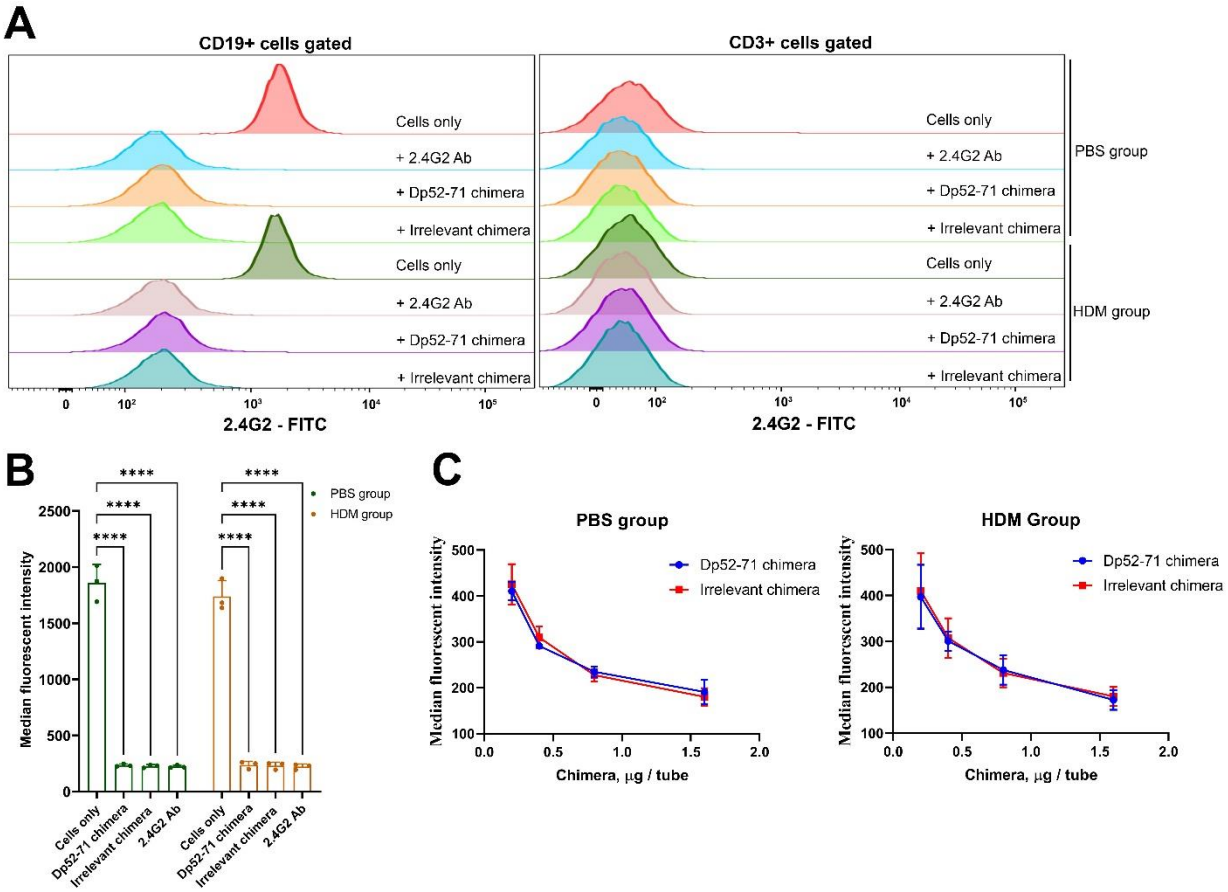


**Figure 7.** The Dp52-71 chimera binds to the FcγRIIb receptor on mouse B cells. (A) Dp52-71 and irrelevant chimera compete with commercially available 2.4G2-FITC antibody for the FcγRIIb receptor. Splenocytes from healthy and HDM-stimulated mice were pre-incubated with Dp52-71 chimera, irrelevant chimera, and pure 2.4G2 antibody, then secondary incubated with 2.4G2-FITC antibody. Isolated CD19 and CD3 cell populations were analyzed by FACS. (B) Summary data for binding of 2.4G2-FITC to the FcγRIIb receptor on B cells. (C) Dose-dependent inhibition of binding of 2.4G2-FITC to the FcγRIIb receptor. Data are presented as mean ± SD from at least 3 mice per group. Differences between groups were assessed using two-way ANOVA followed by Tukey's multiple comparisons test; ****p<0.0001.

Both chimera molecules and the pure 2.4G2 antibody showed similar capacity to engage the FcγRIIb receptor, effectively preventing the binding of the commercial 2.4G2-FITC antibody to CD19 cells (Figure 7A, B). The observed inhibition of binding was dose-dependent (Figure 7C).

The presence of Der p 1 peptide epitopes on the Dp52-71 chimera was confirmed by ELISA analysis. It was found that serum IgG1 antibodies from animals sensitized with HDM+Alum recognized the Dp52-71 chimera to a greater extent compared to the irrelevant chimera (Figure 8).

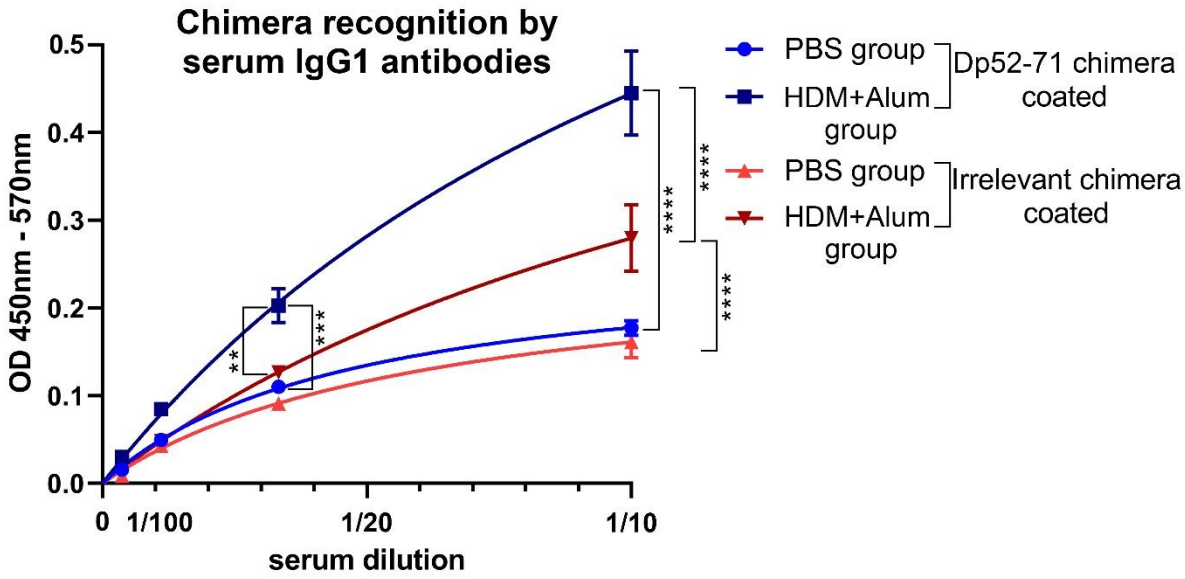


**Figure 8.** The Dp52-71 chimera is recognized by epitope-specific serum IgG1 antibodies. The recognition of the peptides from the Dp52-71 chimera by serum IgG1 antibodies from HDM+Alum-sensitized mice was analyzed by ELISA. The data are presented as the mean ± SD from at least 3 mice per group. Differences between groups were evaluated using a two-way ANOVA test followed by Tukey's multiple comparisons test; **p<0.01; ***p<0.001; ****p<0.0001.

### 2.2. Serum levels of HDM-specific and total IgE antibodies

A chronic mouse model of house dust mite allergy was developed to assess the effects of chimera molecules on the manifestation of allergic inflammation (Figure 9A). The experimental mice were randomly divided into four groups. The control group of healthy animals was treated i.n. and i.v. with PBS (PBS group), while the remaining three groups were sensitized and stimulated i.n. with HDM extract. The HDM-sensitized animals were injected i.v. with PBS (HDM group), Dp52-71 chimera (HDM + Dp52-71 chimera group), or irrelevant chimera (HDM + irrelevant chimera group).

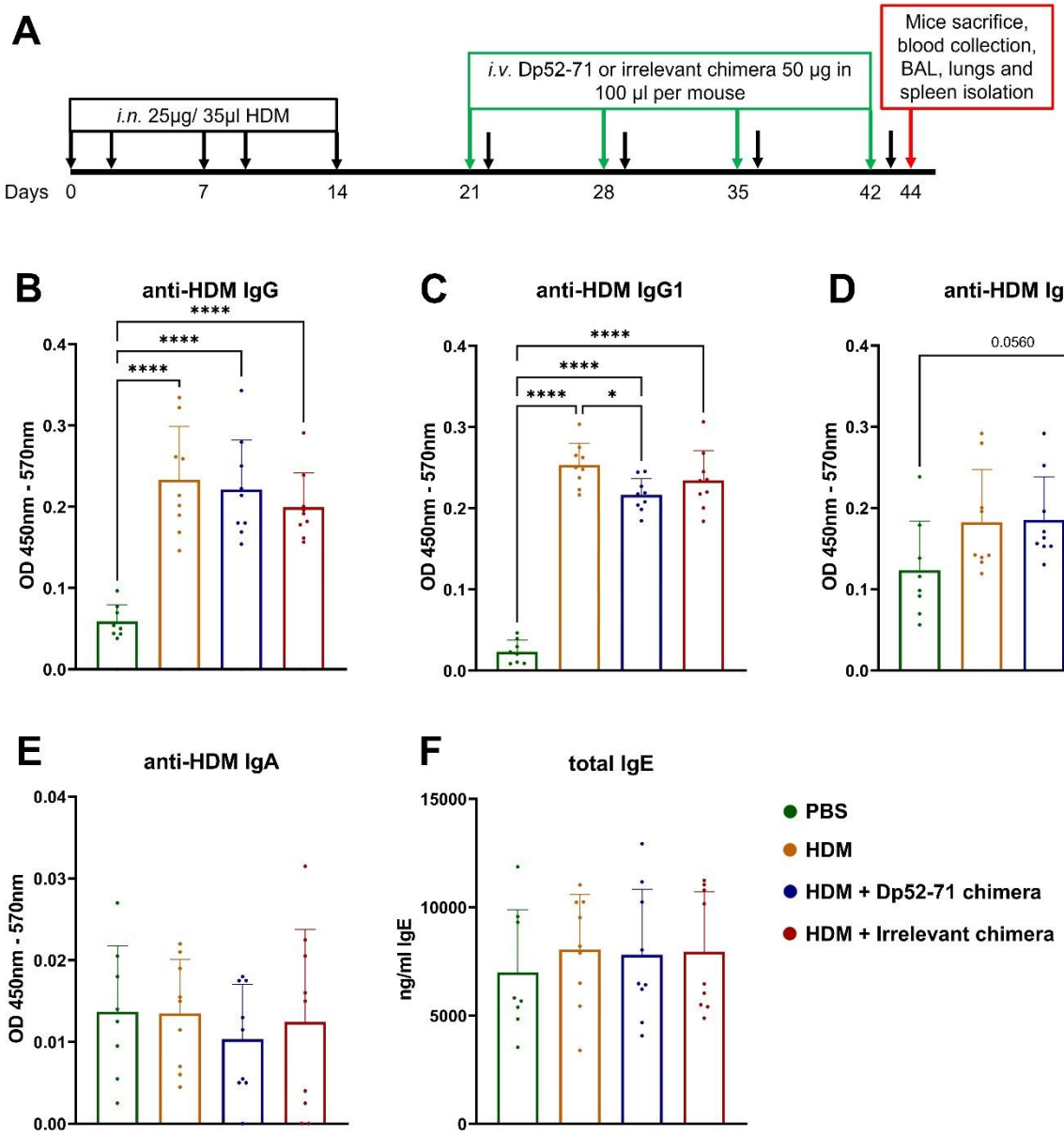


**Figure 9.** Scheme of chronic HDM allergy mouse model and treatment regimen (A). ELISA analysis of serum levels of anti-HDM IgG (B), IgG1 (C), IgM (D), IgA (E), and total IgE antibodies (F) in healthy mice and HDM-sensitized mice treated with PBS, Dp52-71 chimera, or irrelevant chimera. The data are presented as mean ± SD from 8-9 mice per group. p-values were calculated using one-way ANOVA followed by Tukey's multiple comparisons test; *p<0.05; ****p<0.0001.

The effect of the chimeric molecules on allergen-specific antibody levels in mouse sera was assessed by ELISA analysis. Levels of HDM-specific IgG and IgG1 antibodies were elevated in the groups treated with HDM compared to the PBS group (Figure 9B, C). Treatment with Dp52-71 chimera led to a statistically significant reduction in anti-HDM IgG1 antibody levels compared to the HDM group (Figure 9C). This effect was not observed in the mice treated with

irrelevant chimera. No statistically significant differences were found in anti-HDM IgG antibody levels between the HDM group and the two chimera-treated groups (Figure 9B).
The HDM-treated groups did not show statistically significant increases in serum HDM-specific IgM antibody levels compared to the PBS-treated mice (Figure 9D). However, a trend toward an increase was observed, reaching its greatest difference in the irrelevant chimera-treated group (p-value = 0.056). No significant differences were found between groups in serum levels of HDM-specific IgA (Figure 9E) and total IgE antibodies (Figure 9F). HDM-specific IgE antibodies were examined by high-sensitivity fluorescent ELISA analysis. No differences were observed in the levels of anti-HDM IgE antibodies between the healthy controls and HDM-treated mice (data not shown).

### 2.3. Analysis of proteins in BALF

We investigated several key proteins in BALF samples to assess the characteristics of the local immune response. The total protein concentration in BALF was used as a marker for vascular permeability [176,179]. Another important parameter is mast cell degranulation in the lungs, which can be measured by analyzing β-hexosaminidase activity in BALF [176,180]. Both total protein concentration (Figure 10A) and β-hexosaminidase enzyme activity (Figure 10B) were elevated in all HDM-treated groups. A trend towards reduced protein concentration and β-hexosaminidase activity was observed in HDM-sensitized animals treated with either Dp52-71 or irrelevant chimera, compared to the HDM group.

Mice in the HDM group showed elevated levels of the cytokine IL-5 (Figure 10C), anti-HDM IgG (Figure 10E), and IgG1 antibodies (Figure 10F) compared to the healthy control group.

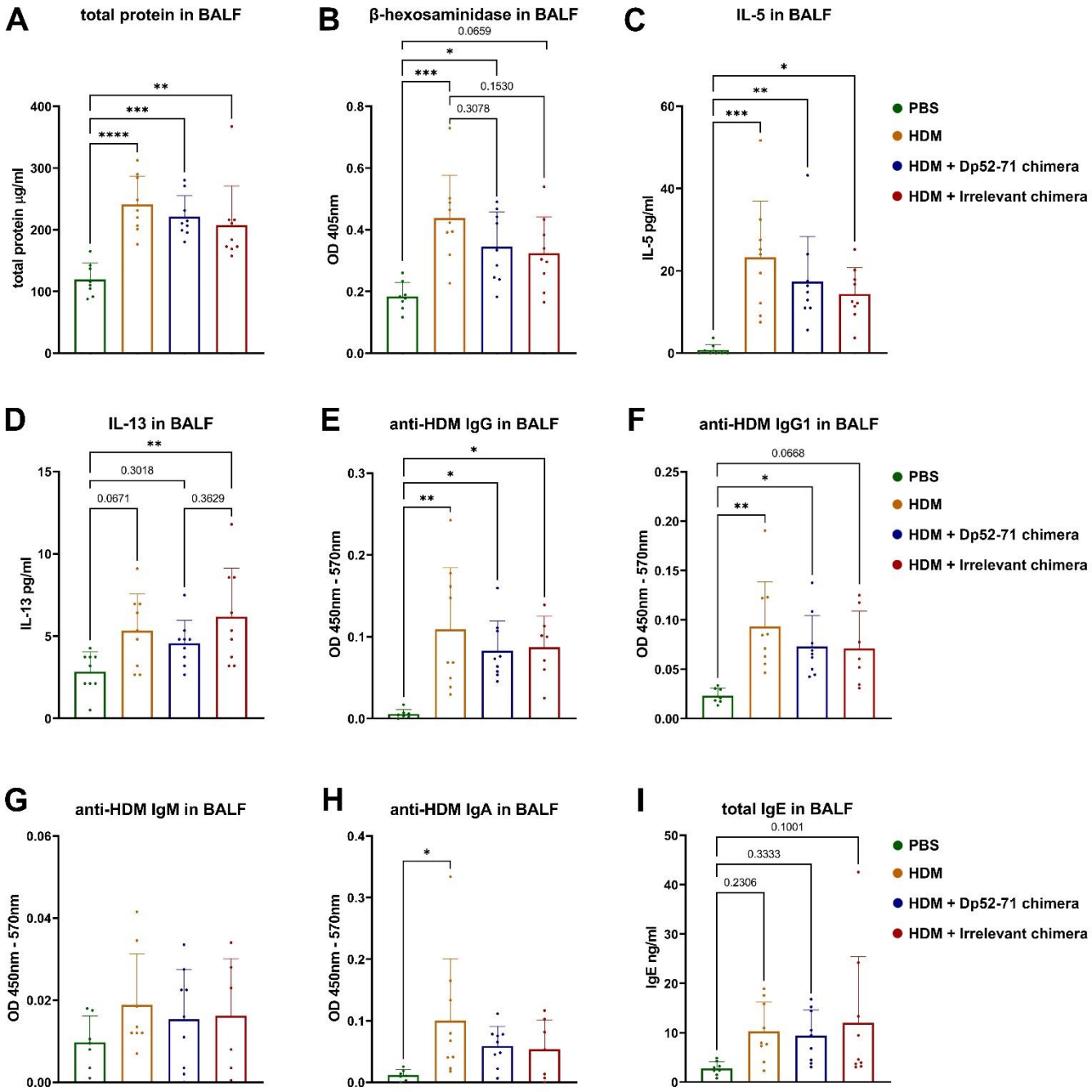


**Figure 10.** Protein analysis in BALF samples. The levels of total proteins (A), β-hexosaminidase activity (B), IL-5 (C), IL-13 (D), HDM-specific IgG (E), IgG1 (F), IgM (G), IgA (H), and total IgE antibodies (I) in BALF were analyzed in all groups. Data are presented as mean ± SD from 6-9 mice per group. Differences between groups were assessed using one-way ANOVA followed by Tukey's multiple comparisons test; p-values are indicated on the graphs, *p<0.05; **p<0.01; ***p<0.001; ****p<0.0001.

It was observed that these parameters were reduced in the groups treated with Dp52-71 or irrelevant chimera compared to the HDM group, but the difference was not statistically significant. The concentration of IL-13 in BALF samples was higher in the irrelevant chimera group compared to healthy animals, but a similar statistically significant difference was not

observed in the Dp52-71 chimera-treated group (Figure 10D). Elevated levels of anti-HDM IgA antibodies in BALF were observed in the HDM-stimulated group compared to PBS mice (Figure 10H). No statistically significant differences were observed between groups in the levels of HDM-specific IgM (Figure 10G) and total IgE antibodies (Figure 10I), nor in the cytokines IL-4 and IL-9 (data not shown).

### 2.4. Total and differential cell count in BAL

Analyses of the total and differential cell counts in BAL were performed to track the local cellular immune response following stimulation with HDM allergens. The total number of isolated cells from the lungs was significantly higher in the HDM group compared to PBS-treated animals (Figure 11B). A partial decrease in this parameter, without statistical significance, was observed in the groups treated with Dp52-71 or irrelevant chimera. All groups treated with HDM showed an increased total cell count in BAL compared to the PBS-treated animals (Figure 11C). A trend, without statistical significance, for a lower number of cells in BAL was found in the group treated with irrelevant chimera ($p = 0.2686$). No difference was found in the number of splenocytes isolated between the experimental groups (Figure 11A).

Differential staining and cell counting in BAL showed a lower percentage of macrophages in all HDM-treated groups compared to PBS-treated mice (Figure 11D). An increased percentage and cell count of neutrophils (Figure 11E, I), eosinophils (Figure 11G, K), and lymphocytes (Figure 11J) were found in the HDM-stimulated groups compared to healthy mice. No statistically significant differences were observed in these parameters between the HDM-treated groups.

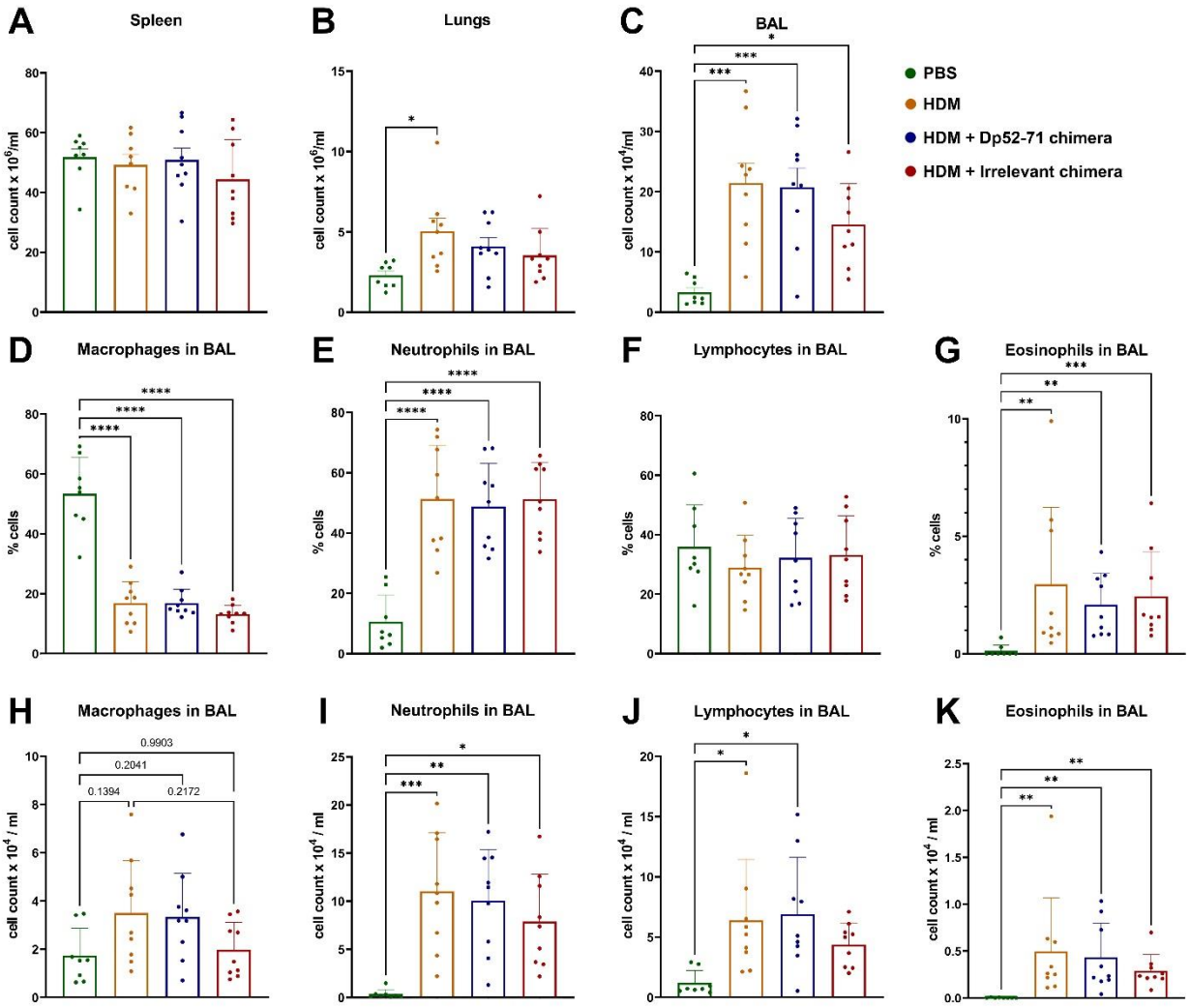


**Figure 11.** Total cell count (per milliliter) isolated from spleen (A), lungs (B), and BAL (C). Differential cell staining in BAL showing macrophages (D, H), neutrophils (E, I), lymphocytes (F, J), and eosinophils (G, K), expressed as percentages and cell counts per ml of recovered BAL fluid. Data are presented as mean ± SD from 8-9 mice per group. Differences between groups were evaluated using one-way ANOVA followed by Tukey's multiple comparisons test or by Kruskal-Wallis test with subsequent Dunn's multiple comparisons test, depending on the normality of the data distribution; p-values are indicated on the graphs, *p<0.05; **p<0.01; ***p<0.001; ****p<0.0001.

### 2.5. Phenotyping of immune cells in the lungs

Phenotyping was performed through FACS analysis of immune cell populations in the lungs to better characterize the local inflammation (Figure 12).

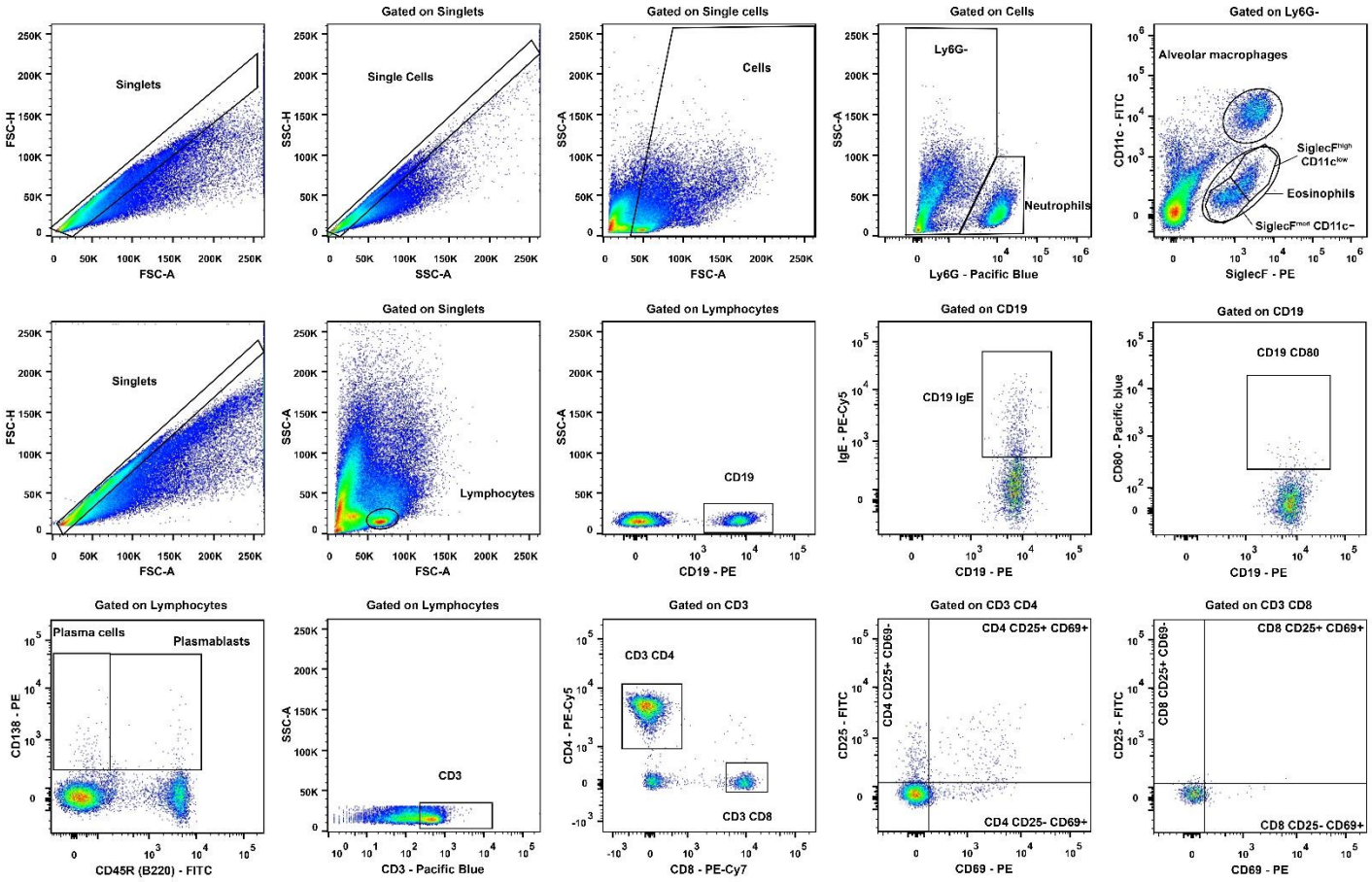


**Figure 12.** Gating strategy for defining distinct cell populations in the phenotyping of immune cells in the lungs by FACS analysis. Gating strategy for defining populations of myeloid cells (first row), B cells and antibody-secreting cells (second row), and T cells (third row).

First, we analyzed the phenotype of myeloid cells, which are known to play an important role in this type of inflammation (Figure 13). An increased percentage of eosinophils was found in the lungs of the HDM group and the group treated with the irrelevant chimera compared to healthy control animals (Figure 13 II). Two different populations of eosinophils were identified based on surface markers SiglecF and CD11c. The SiglecF$^{high}$ CD11c$^{low}$ eosinophils, described in the literature as the more activated population, were increased in the HDM-treated groups compared to healthy animals (Figure 13 III). A trend without statistical significance for a lower percentage of these cells was observed in the group treated with the Dp52-71 chimera compared to the HDM group ($p = 0.7483$). No differences were observed between groups in the second identified eosinophil population, characterized as SiglecF$^{med}$ CD11c- (Figure 13 IV), described in the literature as tissue-resident and less activated [181,182]. No differences between groups were found in the population of alveolar macrophages (Figure 13 I). A partial increase without

statistical significance was observed in neutrophils in all groups treated with HDM (Figure 13 V).

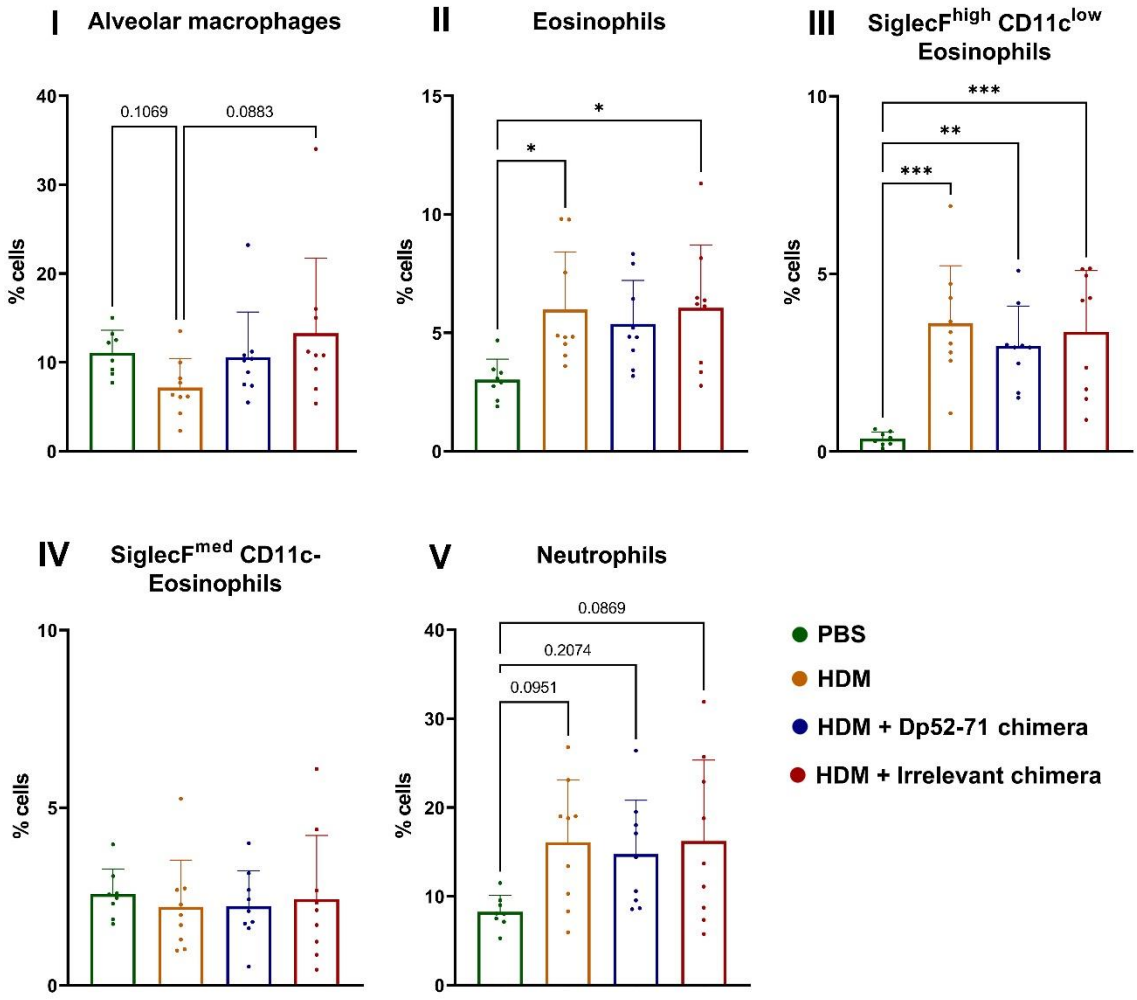


**Figure 13.** Phenotyping of myeloid immune cells through FACS analysis in the lungs. Characterization of different types of myeloid cells – alveolar macrophages (I), SiglecF$^{high}$ CD11c$^{low}$ (III), SiglecF$^{med}$ CD11c- (IV), and total eosinophils (II), and neutrophils (V), presented as a percentage of the parent population. Data are shown as the mean ± SD from 8-9 mice per group. Differences between groups were assessed using one-way ANOVA followed by Tukey's multiple comparisons test or Kruskal-Wallis test with subsequent Dunn's multiple comparisons test, depending on the normality of data distribution; p-values are indicated on the graphs, *p<0.05; **p<0.01; ***p<0.001.

Since the chimeric molecules are targeted at allergen-specific B cells, characterizing this cell type as well as antibody-secreting cells is of great interest for our research (Figure 14). FACS analysis revealed a significantly increased number of CD19+ cells in the HDM group compared to healthy mice (Figure 14 I). A partial increase without statistical significance was observed in the groups treated with Dp52-71 or irrelevant chimera.

The expression of CD32 (FcγRIIb) on B cells is important because it is the target protein recognized by the chimeric molecules. The expression, measured as the mean fluorescent intensity (MFI) of CD32 on CD19 cells (Figure 14 VII), as well as on CD19+ IgE+ cells (Figure 14 VIII), was significantly higher in the HDM group compared to mice treated with PBS. It has been found that in some cases, FcγRIIb can induce inhibitory signals in B cells independently of the B-cell receptor (BCR) [183,184]. The observed overexpression in HDM-stimulated mice may explain similar trends in some parameters in the groups treated with Dp52-71 or irrelevant chimera. The application of Dp52-71 or irrelevant chimera did not affect the expression of CD32 on CD19+ and CD19+ IgE+ cells compared to the HDM group. The percentages of total antibody-secreting cells (CD138 positive cells) (Figure 14 IV) and plasmablasts (Figure 14 VI) were higher in all HDM-stimulated groups compared to the healthy control group. No significant differences were found between the groups in the number of plasma cells (Figure 14 V), CD19+ CD80+ (Figure 14 II), and CD19+ IgE+ (Figure 14 III) expressing cells.

T-cell subtypes in the lungs of HDM-treated mice were also analyzed (Figure 15). The analysis showed a significantly reduced number of CD3+ cells in the HDM group compared to healthy mice (Figure 15 I). However, no differences were found in the percentage of CD3+ CD4+ (Figure 15 II) and CD3+ CD8+ T cells (Figure 15 III). Activated T-cell subtypes CD4+ CD69+ CD25+ (Figure 15 V) and CD4+ CD69+ CD25- (Figure 15 VI) were elevated in all HDM-treated groups compared to control animals. A decrease without statistical significance in these cells was observed in the group treated with Dp52-71 chimera compared to the HDM group (CD4+ CD69+ CD25+, $p=0.7675$; CD4+ CD69+ CD25-, $p=0.4809$). No significant differences were found between the groups in the subpopulations of activated CD8+ cells (Figure 15 VIII, IX).

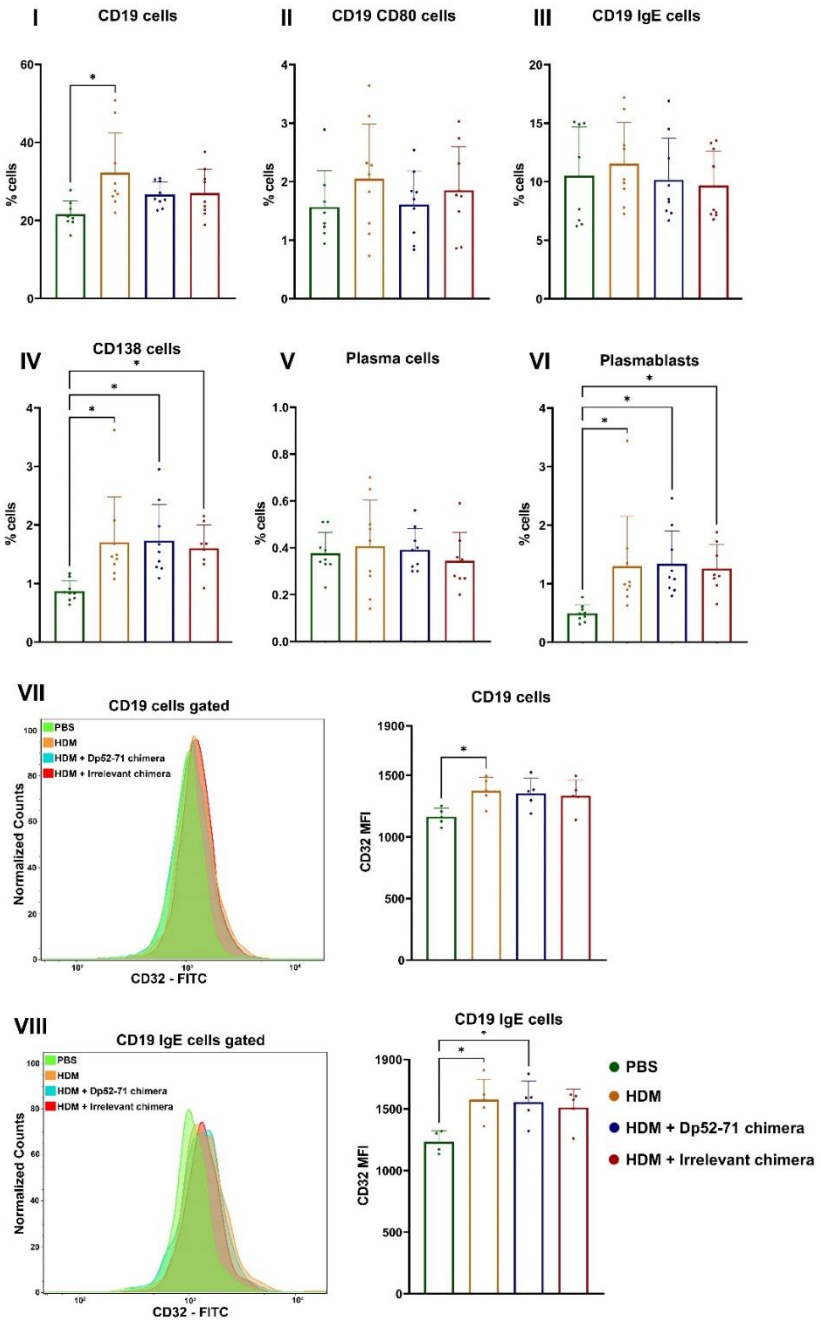


**Figure 14.** Phenotyping of B cells and antibody-secreting cells in lungs by FACS analysis. Summary data are presented for the percentages of CD19 cells (I), CD19 CD80 cells (II), CD19 IgE cells (III), CD138 cells (IV), plasma cells (V), and plasmablasts (VI). Summary data are also presented for the mean fluorescent intensity (MFI) of CD32 on CD19 (VII) and CD19 IgE cells (VIII). Data are presented as the mean ± SD from 8-9 mice per group. Differences between groups were evaluated using a one-way ANOVA test followed by Tukey's multiple comparisons test or by the Kruskal-Wallis test with subsequent Dunn's multiple comparisons test, depending on the normality of the data distribution; p-values are indicated on the graphs, *p<0.05.

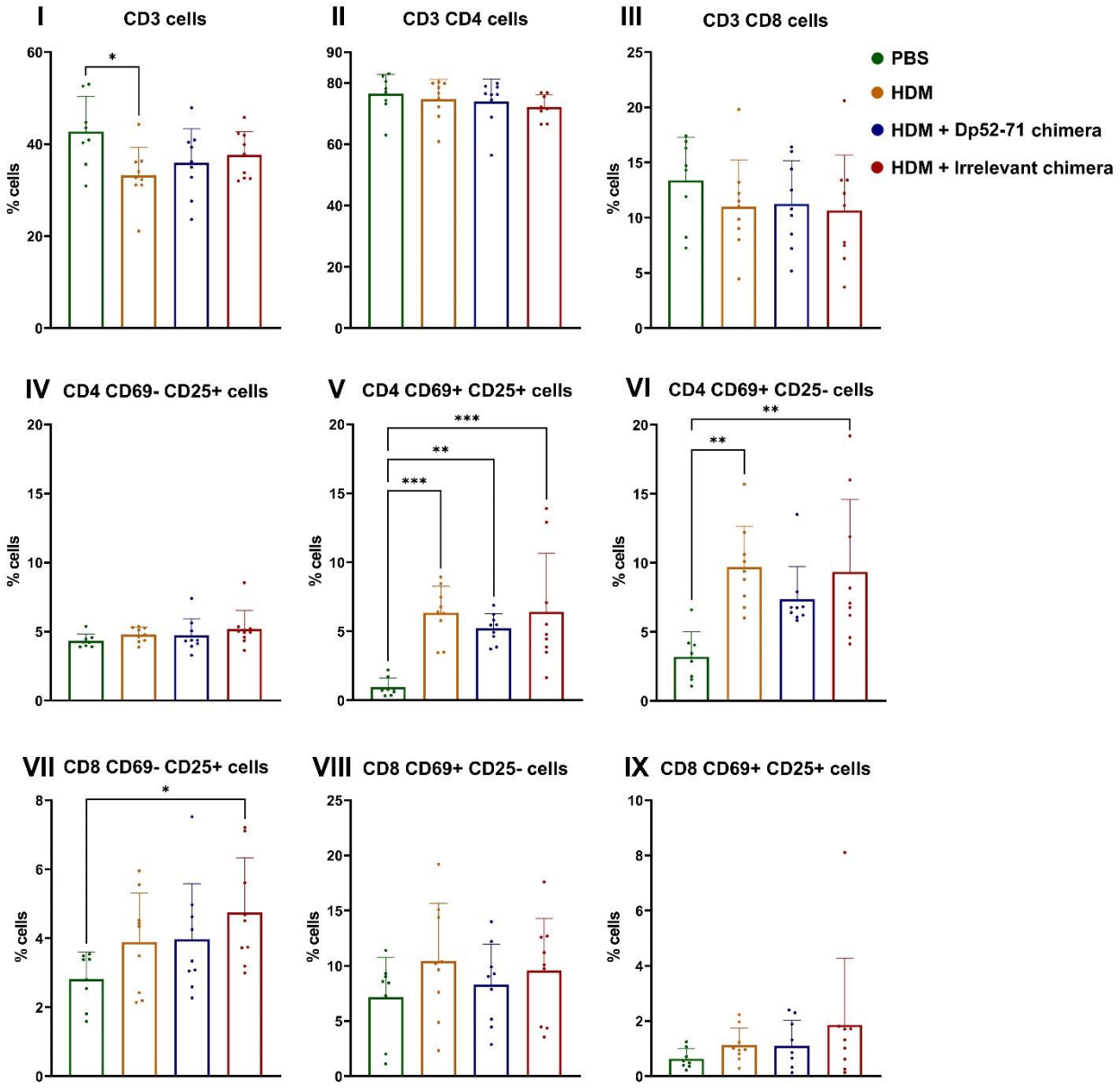


**Figure 15.** Phenotyping of T cell populations in lungs by FACS analysis. Summary data are presented for the percentages of CD3 cells (I), CD3 CD4 cells (II), CD3 CD8 cells (III), CD4 CD69-CD25+ cells (IV), CD4 CD69+ CD25+ cells (V), CD4 CD69+ CD25- cells (VI), CD8 CD69- CD25+ cells (VII), CD8 CD69+ CD25- cells (VIII), and CD4 CD69+ CD25+ cells (IX). Data are presented as the mean ± SD from 8-9 mice per group. Differences between groups were evaluated using a one-way ANOVA test followed by Tukey's multiple comparisons test or by the Kruskal-Wallis test with subsequent Dunn's multiple comparisons test, depending on the normality of the data distribution; p-values are indicated on the graphs, *p<0.05.

### 2.6. Histopathological examination of lungs

Finally, the overall allergic inflammation in the lungs was examined through histological analysis. Hematoxylin and eosin (H&E) staining of mouse lung tissue revealed perivascular

(Figure 16A, D) and peribronchial (Figure 16B, E) cellular infiltration in all HDM-treated groups, with no significant differences observed between the groups.

PAS-positive epithelial cells in the airways, representing goblet cells responsible for mucus production, were found in the airways of the HDM-treated groups but not in healthy mice (Figure 16C, F). A decrease in the histopathological PAS score was observed in the group treated with Dp52-71 chimera compared to the HDM group, with a p-value close to statistical significance ($p = 0.1025$).

### 2.7. Correlation analysis in the HDM group

Although mouse models for inducing HDM allergy have similar protocols, the outcome of their allergic inflammation often differs [185]. To better characterize our HDM allergy model and the relationships between the individual parameters studied, we performed a correlation analysis within the HDM group. This additional data analysis can help us better understand the connection between the immunological parameters of interest. Figure 9C shows that the application of the Dp52-71 chimera leads to a decrease in HDM-specific IgG1 antibody levels in the serum. However, the impact of the Dp52-71 chimera on other immunological parameters is either absent or weak, which is insufficient to reach statistical significance. Therefore, we performed a correlation analysis to explore how anti-HDM IgG1 antibodies are related to parameters indicating allergic inflammation. A strong statistically significant positive correlation was found between serum levels of anti-HDM IgG1 antibodies and the total protein concentration in BALF, the enzyme activity of β-hexosaminidase in BALF, the percentages of $SiglecF^{high}$ $CD11c^{low}$ eosinophils in the lungs, and the PAS score in the lungs (Figure 17). These results provide a basis for suggesting that the observed trends, which are not statistically significant between the Dp52-71-treated group and the HDM group, may result from the weak effect generated by targeting B cells specific only to one epitope that is part of only one allergen.

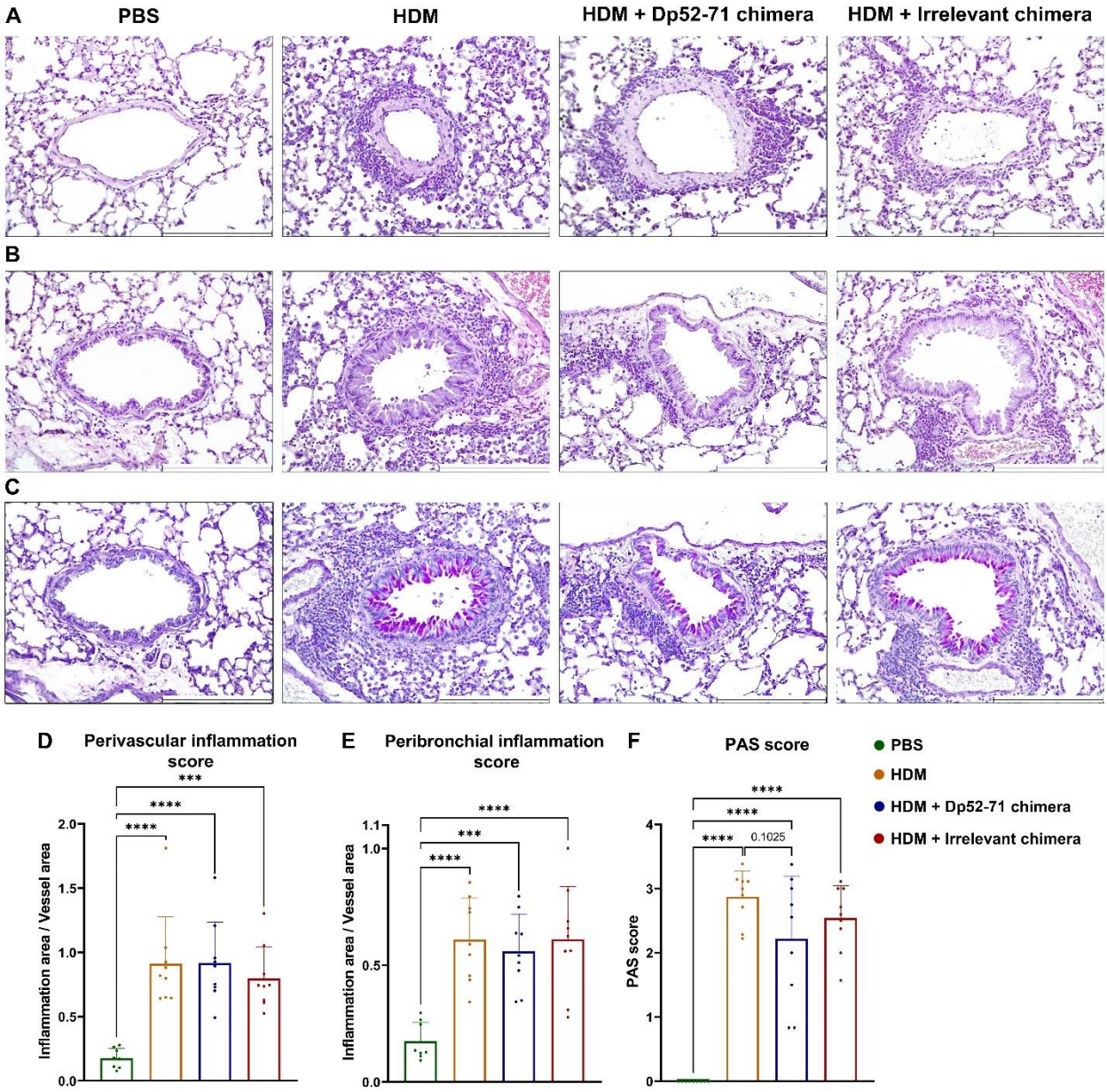


**Figure 16.** Histopathological analysis of the lungs. Representative images and histological assessment (score) of perivascular (A, D) and peribronchial (B, E) inflammation of lung tissue stained with H&E, PAS score (F), and representative images showing mucus secretion (C). Scale bar size, 250 µm. Data are presented as mean ± SD from 8-9 mice per group. p-values were calculated using one-way ANOVA followed by Tukey's multiple comparisons test; p-values are indicated on the graphs, ***p<0.001; ****p<0.0001.

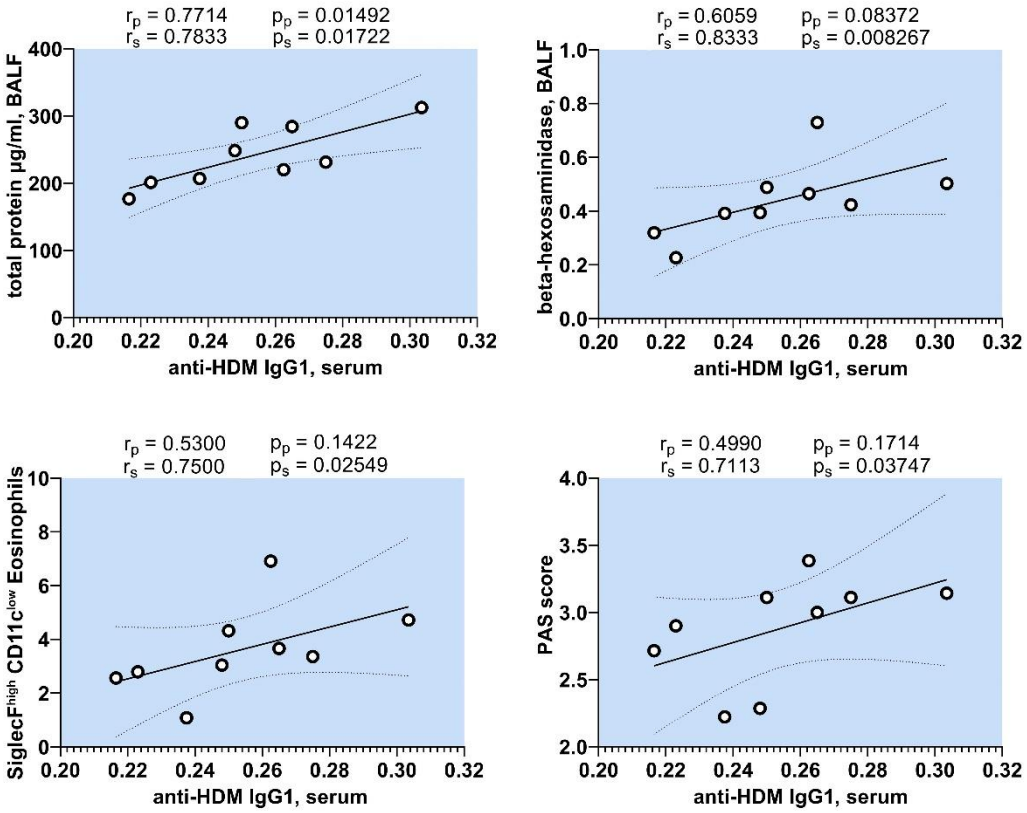


**Figure 17.** Correlation analysis in the HDM group. Correlation analysis of serum levels of anti-HDM IgG1 versus total protein concentration in BALF, β-hexosaminidase enzyme activity in BALF, percentages of SiglecF$^{high}$ CD11c$^{low}$ eosinophils in the lungs, and PAS score of the lungs. The Pearson (rp) and Spearman (rs) correlation coefficients and p-values for the Spearman (ps) and Pearson (pp) correlation analysis are indicated above each figure.

The percentage of SiglecF$^{high}$ CD11c$^{low}$ eosinophils in the lungs showed a positive correlation with β-hexosaminidase and IL-5 in BALF, as well as a strong positive correlation with the PAS score (Figure 18). Interestingly, serum levels of anti-HDM IgG antibodies did not correlate with the parameters that were correlated with anti-HDM IgG1 antibodies.

Another interesting finding in this study is the overexpression of CD32 on the surface of lung B cells in the HDM allergy model. Additionally, we aimed to determine whether this overexpression correlates with other immunological parameters studied in this mouse model. The results showed a significant negative correlation between the CD32 MFI signal on B cells in the lungs and the percentage of alveolar macrophages and neutrophils in the lungs, as well as the concentration of IL-13 in BALF (Figure 19).

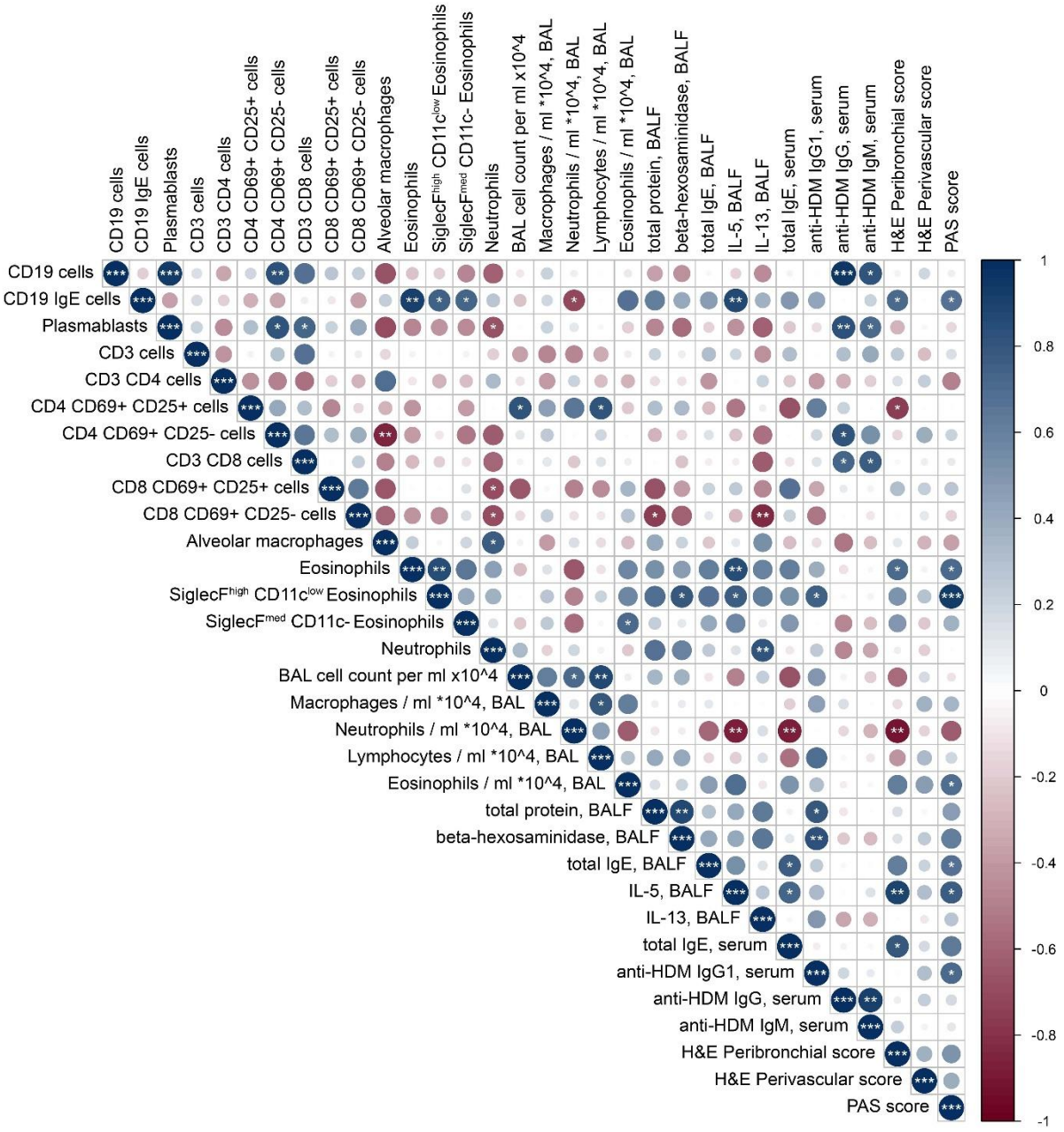


**Figure 18.** Correlation analysis in the HDM group. Correlation matrix of key immunological parameters, performed using the Spearman test (*p<0.05; **p<0.01; ***p<0.001).

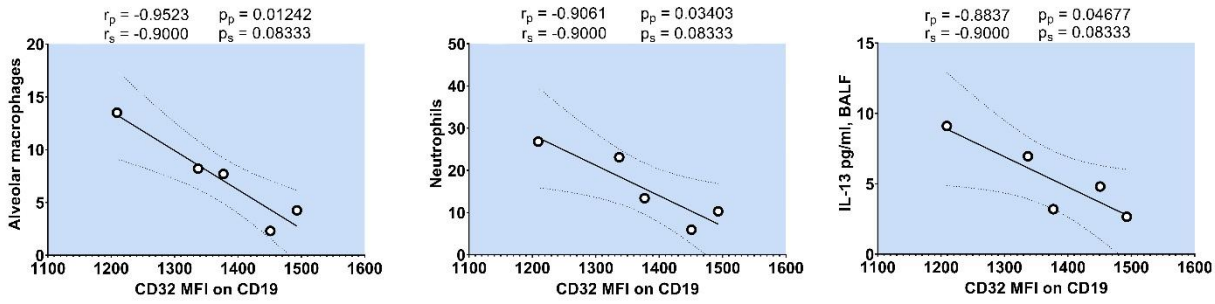


**Figure 19.** Correlation analysis in the HDM group. Correlation analysis of CD32 expression on B cells in the lungs with the percentage of alveolar macrophages and neutrophils in the lungs, as well as IL-13 concentration in BALF. The Pearson (rp) and Spearman (rs) correlation coefficients and p-values for Spearman (ps) and Pearson (pp) correlation analysis are indicated above each figure.

# V. DISCUSSION

## 1. Humanized mouse model of house dust mite allergy

It is considered that the generation of high-affinity IgE antibodies is a key step in allergic diseases, where a small amount of environmental allergen can trigger a very strong hypersensitivity response. It is known that there is a correlation between serum levels of IgE and the number of FcεRI receptors expressed on basophils and mast cells [76,186]. Therefore, eliminating circulating IgE antibodies or IgE-producing B cells as pathological factors in the inflammatory cascade could be a promising therapeutic approach.

Currently, only a few antibody-based therapeutic approaches have been approved for the treatment of allergic patients and reduction of allergic reactions. Patients with allergy and allergic asthma treated with omalizumab show a decrease in tissue eosinophilia and the secretion of inflammatory mediators, as well as a reduction in the number of IgE-positive and FcεRI-positive cells in the submucosa. These patients also show a reduction in the number of IL-4-producing cells and a decrease in the total number of activated CD4 and CD8 T lymphocytes in the respiratory tract. Omalizumab has been approved for the treatment of severe persistent allergic asthma, particularly in patients who do not respond to conventional therapies [187,188]. As an alternative approach for treating allergic diseases, epitope-specific therapeutic strategies have been developed. Chemically modified allergenic epitopes, as well as various carriers, have been tested to modulate the immune response, suppress IgE production, or induce tolerance [189,190].

Another logical therapeutic approach is the inhibition of IgE antibody production by B cells that specifically recognize the allergen. The present study uses this therapeutic strategy by engaging the inhibitory CR1 and allergen-specific B cell receptor through a protein construct capable of crosslinking both structures on the cell membrane. It has been shown that such artificially created bispecific chimeric molecules carrying anti-CR1 antibodies preferentially recognize disease-associated target B cells rather than other CR1-positive cells [165,166].

The inhibitory function of human CR1 has been confirmed by several authors [147,150,165,166]. Józsi et al. demonstrate that aggregated C3, mimicking C3b—the natural ligand for CR1—leads to a reduction in the free Ca2+ levels and inhibits the phosphorylation of cytoplasmic proteins after CR1 binding to BCR-activated lymphocytes [147]. This inhibitory capacity of CR1 has also been demonstrated in patients with systemic lupus erythematosus [148,151,166].

Der p 1, the major allergen from house dust mites, contains several B- and T-cell epitopes involved in inducing the allergic immune response [170–172]. For constructing our chimeric molecule targeting pathological Dpt-specific B cells, we used a small synthetic peptide (p52-71), containing one of the B-cell epitopes from Der p 1, conjugated to an antibody specific to CR1. This immunodominant peptide has been shown to be an effective inducer of cell activation and exhibits its biological activity only in FcεR+-expressing cells from Dpt-sensitive patients [171]. The recognition of the Der p 1 epitope by anti-Der p 1 IgG and IgE antibodies after peptide-antibody conjugation has been established via ELISA and Western blot in previous studies [174].

The molecular mechanism of the intracellular signaling process initiated by CR1 is still unknown. Since the cytoplasmic tail of the receptor is very short, it can be assumed that the receptor molecule cannot transmit signals independently. The signaling mechanism through CR1 has not yet been studied, and no molecule involved in the CR1-mediated blocking of BCR-induced functions in human B cells has been identified. Previous studies have shown that the Dp52-71 chimera triggers a BCR-independent signal via CR1 in B cells isolated from tonsils, leading to the phosphorylation of tyrosine in a protein with an approximate molecular weight of 30–32 kDa. These data suggest the existence of an unknown inhibitory pathway in human B cells, initiated by CR1 binding [176]. Inhibition through CD35 provides an additional regulatory checkpoint, by which immune complexes and C3 degradation products can limit the activation and function of B cells.

Immunodeficient mouse strains such as SCID, NSG, and Rag2- γc- do not develop functional T, B (and NK) lymphocytes, which makes them tolerant to xenogeneic cell transplantation, such as human lymphoid cells, and allows for limited differentiation and maturation [138,139]. Studies have shown that SCID mice transfused with PBMCs from HDM-sensitized patients and subjected to intranasal stimulation with Dpt allergen develop an allergic reaction similar to that in humans: a Th2-mediated response, production of allergen-specific IgE antibodies, and an inflammatory reaction in the respiratory tract. It has been proven that transferring 1 × 10^7 PBMCs is sufficient to produce detectable levels of human IgE antibodies [142–144]. Passive immunization of SCID mice with sera from Dpt-sensitized patients reveals that human IgE antibodies can bind to mouse mast cells, and stimulation with the allergen leads to an immediate type 1 immune response [145].

To investigate the selective elimination or suppression of Der p 1-specific B lymphocytes *in vivo*, we used a model of HDM allergy in humanized Rag2- γc- mice based on protocols for sensitization and stimulation with HDM, applied to intact BALB/c mice [131]. In previous

studies, we demonstrated that chimeric molecules containing Der p 1 peptides are capable of crosslinking Der p 1-specific BCR receptors and CR1 on allergen-specific B cells from HDM-allergic patients, leading to a significant reduction in the number of plasma cells secreting anti-Dpt IgE antibodies *in vitro* [174]. It is expected that the specific therapy with the constructed chimeric antibody would have more advantages *in vivo* due to its bivalent specificity, and thus could selectively suppress pathological Dpt-specific B cells and the production of anti-Dpt IgE antibodies. It was found that in Rag2- γc- mice humanized with PBMCs from HDM-allergic patients and treated with the Dp52-71 chimera, there was a decrease in the levels of Dpt-specific IgE antibodies in BALF, as well as a reduction in the number of human CD45, CD3, and CD4 cells in the lungs compared to animals treated with the control chimera. In contrast, a significantly larger number of human CD8 T cells were found in the mice treated with the Dp52-71 chimera, and data from other authors suggest that the increased population of human IFN-γ-producing CD8 T cells suppresses the Th2 immune response [191].

Since only one epitope (p52-71) was used for constructing the chimeric molecules, it was not possible to suppress all Der p 1-specific B cells recognizing the various different Der p 1 epitopes. The significant reduction in anti-Der p 1 IgE antibodies may be a result of the phenomenon of epitope spreading, which is known in cases of allergy and autoimmunity. For example, the use of a peptide vaccine from the allergen Fel d1 leads to the induction of an immune response to Fel d1 epitopes not included in the vaccine [192]. This phenomenon may also explain the significant reduction in other monitored clinical parameters.

The investigation of the local immune response in BALF after treatment with the Dp52-71 chimera showed significantly reduced levels of human anti-Dpt IgE antibodies, but not levels of allergen-specific IgA, IgG, and total IgE antibodies compared to the control chimera. Significantly reduced levels of β-hexosaminidase and the concentration of total protein in BALF were also found after treatment with the Dp52-71 chimera, suggesting local inhibition of mast cell degranulation and vascular permeability (Figure 20).

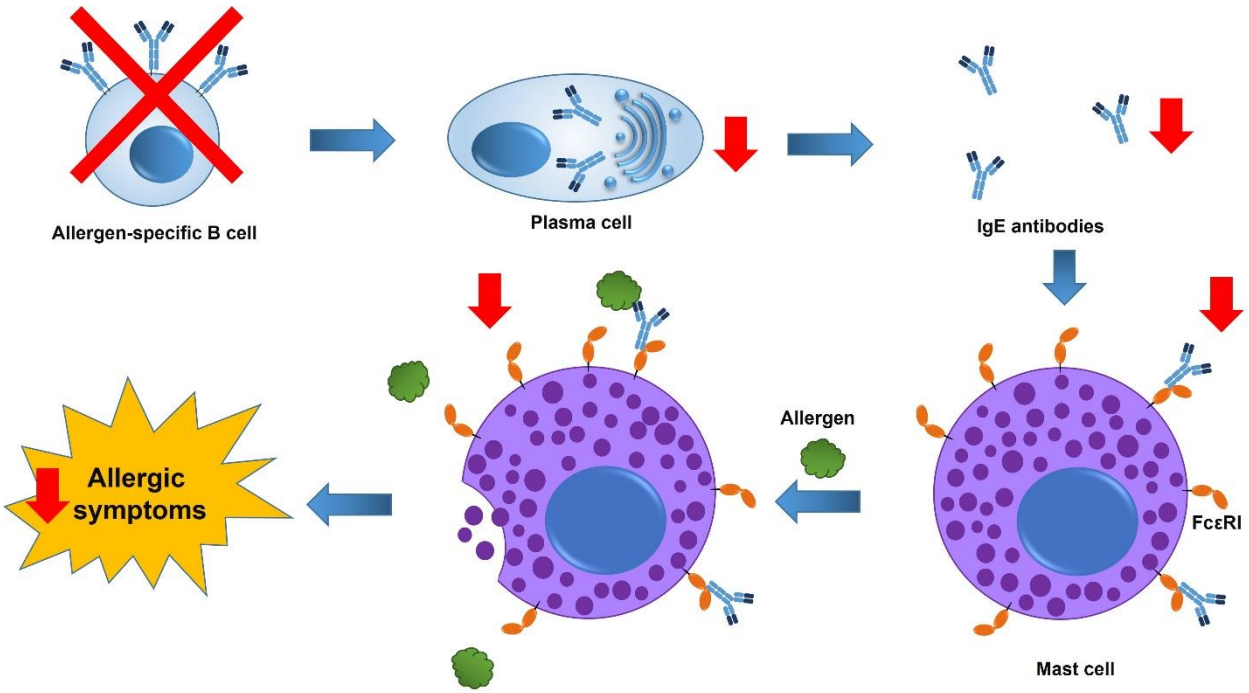


**Figure 20.** Effect of the human Dp52-71 chimeric molecule in the humanized HDM allergy model and proposed mechanism of action.

The Dp52-71 chimera likely inhibits the differentiation of B cells into plasmablasts, but it appears that some existing Dpt-specific antibody-producing plasmablasts are unaffected due to the absence of BCR. Previous studies have shown that the control chimera does not suppress Dpt-specific cells [174]. Importantly, a reduced cellular infiltration was observed in the histopathological evaluation of lungs from animals treated with the epitope-specific chimera. It seems that targeted suppression of Dpt-specific B cells also impairs their antigen-presenting functions, leading to a reduction in pulmonary inflammation.

In the present study, we investigated a protein-engineered CR1-specific chimeric monoclonal antibody in a humanized Rag2- γc- model of HDM allergy to explore a potential new approach for specific therapy. The activity of target Der p 1-specific B cells may be suppressed either by blocking B cell differentiation into IgE-secreting plasma cells or by limiting the pathological communication between T and B lymphocytes. Using these chimeric molecules in a humanized model system, we demonstrate that this approach is effective and has the potential to be further developed to reduce the production of pathological IgE antibodies and histopathological changes in the lungs.

## 2. Chronic murine model of house dust mite allergy

The aim of the present study was to target allergen-specific B cells in a chronic murine model of HDM allergy using a protein-engineered chimeric molecule capable of simultaneously binding BCR and CD32, as a potential new therapeutic approach. Chimeric molecules were constructed consisting of the monoclonal 2.4G2 antibody recognizing FcγRIIb, linked to proven epitope-bearing peptides (p52-71) or control peptides. The newly constructed chimeric molecules retained the ability to bind FcγRIIb on B cells and were recognized by allergen-specific IgG1 antibodies. Administration of the Dp52-71 chimera led to reduced levels of HDM-specific IgG1 antibodies in the serum of mice subjected to chronic intranasal HDM extract stimulation. However, the reduction in antibody levels was partial, likely due to the targeting of a limited epitope-specific B cell population, while the antibody repertoire against the various allergens in the HDM extract is much broader. Additionally, some trends were observed, without statistical significance, in the reduction of several parameters, including β-hexosaminidase in BALF, SiglecF$^{high}$ CD11c$^{low}$ eosinophils in the lungs, with the highest level of significance reached in the pulmonary PAS score (p=0.1025). The Dp52-71 chimera was designed to target mature epitope-specific B cells by simultaneously crosslinking BCR and FcγRIIb and subsequently triggering phosphorylation of the ITIM domain of FcγRIIb. This phosphorylation would lead to the binding of the SH2-domain-containing inositol phosphatase SHIP1, which inhibits activating signals by dephosphorylating the cytoplasmic domain of BCR. However, SHIP- and ITIM-independent signaling through FcγRIIb in the absence of BCR signaling can induce apoptosis in mature B cells through activation of pro-apoptotic proteins BAD and BID. Moreover, the outcome of signaling through FcγRIIb also depends on the developmental stage of the B cells. While simultaneous crosslinking of FcγRIIb and BCR inhibits proliferation of mature B cells and pro-B cells, isolated binding to FcγRIIb leads to apoptosis in activated B cells, pre-B cells, and plasma cells [157,193]. Although the Dp52-71 chimera could bind non-target cells to some extent, it preferentially binds to Dp52-71-specific B cells due to the increased overall avidity, equivalent to the sum of the binding affinities of the peptide to BCR and the 2.4G2 antibody to FcγRIIb.

A series of studies, some of which are presented in the current dissertation (humanized model), track the *in vitro* and *in vivo* effects of chimeric molecules targeting the same Dp52-71-specific B cell population in patients with HDM allergy and the inhibitory receptor CR1. Treatment with these anti-human CR1 chimeric molecules, containing the same epitope-bearing peptides as the murine chimera, reduces the number of anti-HDM IgE-secreting cells and induces B cell

apoptosis *in vitro* [174]. Administration of the anti-human chimeric molecule in a humanized Rag2- γc- model of HDM allergy results in a decrease of HDM-specific IgE antibodies both in the serum and in BALF. This treatment also reduces levels of total protein and β-hexosaminidase in BALF, as well as immune cell infiltration in the lungs [176]. Although both murine and human chimeric molecules lead to a reduction in HDM-specific antibodies, the results of the treatment on overall allergic inflammation differ, as the murine chimeras fail to achieve statistically significant reductions in other disease parameters. The reason for this discrepancy may be due to various factors, such as the specificity of the target receptors, as well as the characteristics of the humanized and murine models. It is possible that the immune response levels against the immunodominant allergen Der p 1, and particularly against the p52-71 peptide, differ between allergic disease in humans and the chronic murine HDM allergy model. Furthermore, the observed trends, which lack statistical significance, between the Dp52-71 chimera group and the HDM group align with parameters that show a strong positive correlation with anti-HDM IgG1 antibodies in the HDM group (β-hexosaminidase in BALF, SiglecF$^{high}$ CD11c$^{low}$ eosinophils, and PAS score in the lungs). Based on these results, it is tempting to speculate that the reduction in HDM-specific IgG1 antibody levels may be related to the trends observed between the Dp52-71 chimera group and the HDM group, addressing the lack of statistical significance in these parameters due to the small effect size generated by targeting B cells specific only to a single allergenic epitope.

The present study investigates a new therapeutic strategy to target allergen-specific B cells using chimeric molecules. A chronic murine model of HDM allergy was developed to assess the *in vivo* effects of the proposed therapy. This HDM allergy model was characterized by elevated serum levels of HDM-specific IgG and IgG1 antibodies. However, no differences were observed in the levels of total and HDM-specific IgE antibodies between healthy and HDM-treated mice. Some studies using murine models of HDM allergy have succeeded in inducing HDM-specific IgE antibodies, but this increase is often very weak compared to that seen in HDM-sensitive allergic asthma patients [194]. Other authors using murine HDM allergy models focus on analyzing HDM-specific IgG1 antibodies and either do not measure anti-HDM IgE antibody levels or fail to detect elevated levels of allergen-specific IgE antibodies [134,194–197]. Additionally, studies show that differences in the biochemical composition of HDM extracts, such as protease content, are responsible for total and HDM-specific IgE antibodies but not for anti-HDM IgG1 antibodies [185,198]. Furthermore, experiments involving mice deficient in FcεRIα or IgE suggest that neither FcεRIα nor IgE contribute to respiratory allergic disease in a short 14-day HDM allergy model with high or

limiting allergen doses [199]. The lack of IgE response in our chronic murine HDM allergy model may be attributed to the biochemical composition of the batch of HDM extract used or other factors such as the treatment regimen. Nonetheless, the presence of a Th2-dependent HDM-specific IgG1 response, along with increased pulmonary inflammation and mucus secretion, characterizes the state of allergic asthma.

Animal models of HDM allergy are a valuable tool for studying the pathogenesis of the disease and potential therapeutic interventions. However, the differences between allergic models based on factors such as the biochemical composition of HDM extracts and allergen administration protocols necessitate further in-depth analysis of these models. In this study, we aimed to thoroughly characterize our chronic model by examining both humoral and cellular immune responses. The analyses showed that mice stimulated with HDM extract exhibited an increased number of eosinophils, neutrophils, and lymphocytes in the BAL, as well as elevated percentages of SiglecF$^{high}$ CD11c$^{low}$ eosinophils, CD19+ cells, plasmablasts, and activated CD4+ CD69+ CD25+ T cells in the lungs. In the HDM group, increased levels of total protein, β-hexosaminidase activity, and IL-5 in BALF were also detected, along with high levels of HDM-specific IgG1 and IgG antibodies in both BALF and serum. The murine HDM allergy model was associated with histopathological changes in the lungs, such as peribronchial and perivascular inflammation and goblet cell hyperplasia. Correlation analysis of the immunological parameters in this model revealed an interesting relationship between serum levels of HDM-specific IgG1 antibodies and several key parameters of allergic inflammation. We found a strong positive correlation between HDM-specific IgG1 antibodies and total protein levels, β-hexosaminidase activity in BALF, SiglecF$^{high}$ CD11c$^{low}$ eosinophils in the lungs, as well as the lung PAS score. Importantly, serum levels of anti-HDM IgG antibodies did not show a correlation with these parameters, suggesting that IgG1 antibodies play a distinct role in allergic inflammation. While many authors report elevated levels of HDM-specific IgG1 antibodies and use them as markers for antigen-specific B and T cell clonal expansion, the contribution of this antibody subclass to allergic inflammation remains to be clarified, particularly regarding sensitization to HDM allergens [194]. However, experiments investigating the role of allergen-specific IgG1 antibodies in hypersensitivity reactions to ovalbumin shed light on possible mechanisms. Mice passively sensitized with ovalbumin-specific IgG1 antibodies develop positive reactivity in skin tests and enhanced airway responses, accompanied by increased eosinophil levels in the BAL following airway challenge. Furthermore, passive immunization with ovalbumin-specific IgG2a or IgG3 antibodies is not associated with these reactions [200]. Another study found that in mice, death and most of the

pathophysiological changes associated with active or IgG1-dependent passive anaphylaxis depend on the FcR gamma chain. The authors also suggest that systemic anaphylaxis may be significantly mediated by FcγRIII and IgG1 [201]. Additionally, FcγR-mediated uptake of allergen-specific IgG immune complexes by dendritic cells may contribute to airway inflammation. The authors observed that i.n. administration of ovalbumin-specific IgG immune complexes enhanced Th2 cytokine production, antigen-specific T cell proliferation, eosinophilia, and airway inflammation [203,204]. Elevated serum levels of HDM-specific IgG1 antibodies in our allergy model may contribute to the positively correlating parameters, such as total protein, β-hexosaminidase activity in BALF, SiglecF$^{high}$ CD11c$^{low}$ eosinophils in the lungs, and lung PAS score. The study focused on ovalbumin-specific IgG1 antibodies provides evidence for the role of IgG1 in hypersensitivity reactions, including skin test reactivity, airway responses, eosinophilia, mast cell degranulation, and anaphylaxis. Although Th2-associated allergen-specific IgG1 antibodies may participate in the development of several features of HDM allergy in murine models, more research is needed, as the correlation analysis alone is insufficient for conclusive interpretations.

The investigation of the expression of our target molecule, CD32 (FcγRIIb), showed that this receptor is overexpressed on the surface of CD19+ and CD19+ IgE-positive B cells in the lungs of HDM-stimulated mice compared to healthy animals. This overexpression was unaffected by the administration of FcγRIIb-specific Dp52-71 or irrelevant chimeras. Moreover, the overexpression of CD32 exhibited a statistically significant negative correlation with the percentages of alveolar macrophages and neutrophils in the lungs, as well as the concentration of IL-13 in the BALF. To the best of our knowledge, this is the first study to demonstrate FcγRIIb overexpression on B cells in HDM allergy. Research has shown that immunization of the mother organism with ovalbumin leads to FcγRIIb overexpression in IgM+ B cells in the offspring's spleens in an IL-10-dependent manner [205,206]. Surprisingly, similar immunization of mice prior to conception with *Dermatophagoides pteronyssinus* allergens results in reduced FcγRIIb expression on the offspring's B cells [207]. However, these data cannot be directly compared with our results due to several factors. First, our study demonstrates the direct effect of HDM extract on B cell expression of FcγRIIb, rather than the effect of maternal immunization on the offspring. Additionally, we analyzed local lung B cells, and the allergen administration was intranasal, whereas the aforementioned study used B cells from the spleen and a systemic route of allergen administration. The role of FcγRIIb in allergic diseases is primarily known for its function in effector cells, such as inhibiting IgE-induced mast cell activation [208–210]. However, the expression of FcγRIIb on B cells appears to be

critical for the development of mucosal antigen-induced tolerance, which is disrupted in FcγRIIb-/- mice. The transfer of FcγRIIb-expressing B cells is sufficient to induce Foxp3+ regulatory T cells and suppress antigen-specific T cells. Additionally, FcγRIIb-overexpressing B cells have an increased capacity to induce mucosal T cell tolerance and regulatory T cells in B cell-deficient mice [211]. The HDM-induced overexpression of FcγRIIb on lung B cells in the chronic murine model, along with the negative correlation with the percentage of neutrophils and IL-13 concentration, is intriguing. Therefore, further studies are needed to investigate the role of FcγRIIb on B cells in the context of allergic diseases, particularly HDM sensitization.

Here, we explored a potential new approach for the specific therapy of HDM allergy using protein-engineered molecules that lead to a reduction in HDM-specific antibody levels. A limitation of this study is that we cannot expect to suppress the entire spectrum of allergen-specific B cells in HDM allergy using only one Der p 1 epitope. Nevertheless, the specific suppression of B lymphocytes specific to this epitope provides an opportunity for future multi-epitope approaches. The selective elimination of allergen-specific B cells via chimeric molecules holds promising translational potential and could be further developed into a novel approach for specific therapy. This study suggests the future use of FcγRIIb overexpression and the expansion of chimeric technology by incorporating more epitopes to improve allergic inflammation.

# VI. CONCLUSIONS

**Humanized mouse model of house dust mite allergy**

1. A humanized house dust mite allergy model was established by transferring PBMCs from allergic patients into immunodeficient Rag2- γc- mice, triggering an allergic immune response in the lungs.
2. Treatment of the humanized mice with the human CR1-specific Dp52-71 chimera reduces the levels of anti-HDM IgE, total protein, and β-hexosaminidase in BALF.
3. The human CR1-specific Dp52-71 chimera reduces the number of infiltrated human lymphocytes in the lungs.
4. The human Dp52-71 chimera suppresses overall perivascular inflammation in the lungs of the humanized mice.

**Chronic mouse model of house dust mite allergy**

1. The FcγRIIb-specific Dp52-71 chimeric molecules we constructed bind to the FcγRIIb receptor on mouse B cells and are recognized by allergen-specific IgG1 antibodies.
2. A chronic mouse model of HDM allergy was developed, characterized by elevated levels of anti-HDM IgG1 antibodies, an increased number of disease-specific immune cells in the lungs, and the development of allergy-related pathological symptoms.
3. The levels of allergen-specific IgG1 antibodies in the mouse allergy model showed a strong positive correlation with total protein and β-hexosaminidase activity in BALF, $SiglecF^{high}$ $CD11c^{low}$ eosinophils in the lungs, and the pulmonary PAS score.
4. FcγRIIb is overexpressed on the surface of CD19 and CD19 IgE-positive B cells in the lungs of HDM-stimulated mice.
5. The administration of the Dp52-71 chimera reduces the levels of HDM-specific IgG1 antibodies in the serum.
6. The reduction in β-hexosaminidase in BALF, $SiglecF^{high}$ $CD11c^{low}$ eosinophils in the lungs, and the pulmonary PAS score indicates a trend towards modulating the late allergic local response after the end of therapy.

# VII. CONTRIBUTIONS

**Contributions with fundamental scientific significance**

- It is shown for the first time that FcγRIIb is overexpressed on the surface of B lymphocytes, including IgE-positive B cells, isolated from the lungs of mice stimulated with house dust mite allergens.
- A correlation between serum levels of anti-HDM IgG1 antibodies and certain parameters of allergic inflammation has been discovered, which may help clarify the role of IgG1 antibodies in the pathogenesis of mouse models of HDM allergy.

**Contributions with applied scientific significance**

- Experimental humanized and chronic mouse models of house dust mite allergy have been developed, which can be used in studies related to the mechanisms of the disease, as well as new therapeutic approaches.
- The protein-engineered chimera technology used, aimed at selectively eliminating allergen-specific B cells, has the potential to be applied in the development of new approaches for targeted therapy.

# VIII. PUBLICATIONS AND PARTICIPATIONS IN SCIENTIFIC FORUMS

**Publications related to the dissertation:**

1. **Ralchev, N.R.**, Kerekov, N., Mihaylova, N., Kremlitzka, M., Hristova, D., Dzhorev, J., Erdei, A. and Tchorbanov, A.I.. Targeted suppression of Dpt-specific B cells in humanized Rag2-γc-mouse model of HDM allergy. 2022. Scandinavian Journal of Immunology, p.e13241. - **Journal Rank: JCR – Q2; Impact Factor –3.7 (2022)**
2. **Ralchev, N.,** Bradyanova, S., Kerekov, N., Tchorbanov, A. and Mihaylova, N., 2024. Suppression of Pathological Allergen-Specific B Cells by Protein-Engineered Molecules in a Mouse Model of Chronic House Dust Mite Allergy. International Journal of Molecular Sciences, 25(24), p.13661. – **Journal Rank: JCR - Q1; Impact Factor – 4.9 (2023)**

**Participation in scientific events related to the dissertation:**

1. Jubilee Conference "15 Years of the Bulgarian Association of Clinical Immunology", November 6-7, 2020, Hilton Hotel, Sofia; Poster
2. 6th European Congress of Immunology, September 1-4, 2021, virtualeci2021.com; Presentation
3. XVI Working Meeting "Biological Activity of Metals, Synthetic Compounds, and Natural Products", November 24-26, 2021, Sofia; Presentation
4. 3rd Interdisciplinary PhD Forum, June 6-7, 2022, Kyustendil; Presentation
5. 4th Interdisciplinary PhD Forum with International Participation, May 16-19, 2023, Sandanski, Bulgaria; Presentation
6. 18th International Congress of Immunology (IUIS 2023), November 27 - December 2, 2023, Cape Town, South Africa; Poster
7. 7th European Congress of Immunology, September 1-4, 2024, Dublin, Ireland; Presentation
8. Annual Immunology Conference, December 13, 2024, "Rosslyn Central Park" Hotel, Sofia; Presentation
9. STAPA RETREAT, November 25-28, 2024, Sofia; Presentation

Information and Communication Sciences and Technologies

Energy Resources and Energy Efficiency

Nanosciences and New Materials and Technologies

**Biomedicine and Quality of Life**

Biodiversity, Bioresearch and Ecology

Climate Change, Risks and Natural Resources

Astronomy, Space Research and Technologies

Cultural-Historical Heritage and National Identity

Human and Society

## Nikola Ralchev Ralchev, 2025